Government of Kingdom of Denmark
Ministry of Foreign Affairs
Danida
Ref No: 104.Botswana.1.MFS.8

Government of Republic of Botswana
Department of Environmental Affairs
Department of Water Affairs
Harry Oppenheimer Okavango Research Centre

Okavango Delta Management Plan

Hydrology and Water Resources

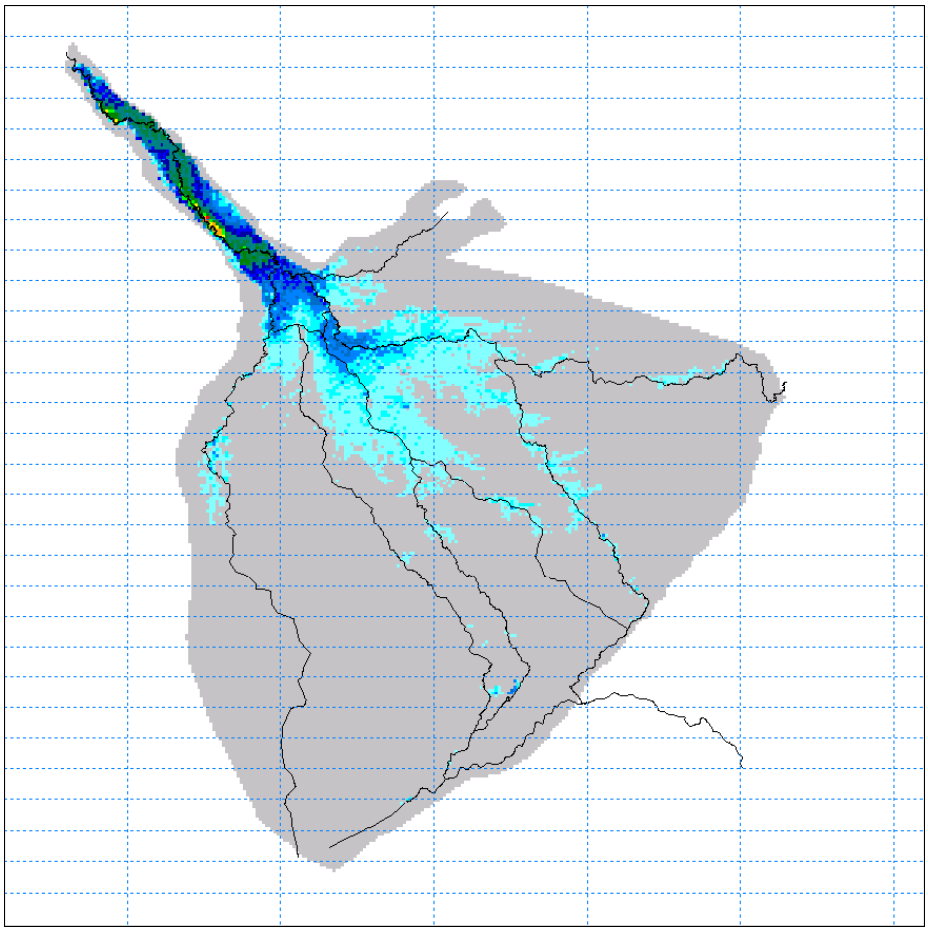

Integrated Hydrologic Model

December 2005

Scanagri Denmark A/S
DHI Water and Environment
Hedeselskabet
Geographic Resource Analysis and Science A/S
Engineering Hydrological and Environmental Services

OKAVANGO DELTA MANAGEMENT PLAN
HYDROLOGY AND WATER RESOURCES
INTEGRATED HYDROLOGIC MODEL
December 2005

List of Contents

List of Contents (cont)

List of Figures

List of Tables

1. INTRODUCTION

The Okavango Delta Management Plan (ODMP) project includes a Hydrology and Water Resources component. An integrated hydrologic model is developed to assist in understanding the hydrologic processes in the delta, and in assessing the impact of alternative management scenarios. In addition, technology transfer to DWA and training the staff of the DWA Modelling Unit have been carried out.

The model development work was initiated in March 2004 and completed in March 2005. Following comments received from various sources, experience applying the model in DWA, and the availability of more recent data for boundary conditions and calibration, the model has been revised with a simpler evapotranspiration routine and an extended calibration period.

The model development has been headed by DHI, but has also involved the DWA Modelling Unit. The hydrologic model is transferred to DWA for future use including a series of scenario analyses to support the ODMP.

2. ABOUT THIS REPORT

This report describes and documents the development and calibration of the Okavango Delta Management Plan Integrated Hydrologic Model. The overall objectives of the project and the specific objectives associated with the model development are initially outlined.

A brief review of the Okavango Delta hydrology highlighting key figures and characteristics is followed by a conceptual approach defining the key processes to address in order to account for the large scale hydrologic responses of the delta.

The conceptual model forms the basis for the development of the Integrated Hydrological Model. Chapter 4 is devoted to discussing the key hydrologic characteristics of the Okavango Delta and identifying the major processes to be considered.

The conceptual model is implemented in a numerical model (MIKE SHE and MIKE 11). The development of the ODMP Integrated Hydrologic Modelling system is covered in chapter 5. The theoretical basis as well as input data are described.

Before applying the ODMP hydrological model, a general assessment of model performance and model calibration has been undertaken. The calibration strategy and calibration results are presented and discussed in chapter 6.

Finally conclusions and recommendations sum up the work and the results highlighting the main model application potential and limitations.

3. OBJECTIVES

The objective of the ODMP project is improved integrated resource management for the Okavango Delta that will ensure its long term conservation, and that will provide benefits for the present and future well-being of the people, through sustainable use of its natural resources. Immediate objectives are:

- A comprehensive, integrated management plan for the conservation and sustainable use of the Okavango Delta and surrounding areas
- Existing data, information and knowledge available in appropriate formats and a timely manner to support the development and initiated implementation of the Okavango Delta Management Plan
- Improved water resources planning, monitoring and evaluation in the Okavango Delta, based on an enhanced capacity of the Department of Water Affairs

The Hydrology and Water Resources component of the project aims at improving water resources planning, monitoring and evaluation in the Okavango Delta, based on an enhanced capacity in the Department of Water Affairs.

One specific output is an Integrated Hydrologic Model of the delta, which will enable analysis of the Okavango waters (NCSA, 2002). The model is being developed using the MIKE SHE–MIKE 11 software from DHI Water and Environment. The model integrates the following four components:

- Soil-vegetation-atmosphere transfer module, describing, in space and time, the loss of water from open water, swamp and terrestrial vegetation to the atmosphere
- MIKE 11 surface water module describing water levels and flows through the main river channels of the delta
- The distributed overland flow module (MIKE SHE) to simulate the two dimensional flow pattern through the swamps and flood plains, with a full automatic coupling with MIKE 11
- MIKE SHE ground water module, based on a three dimensional representation of saturated and unsaturated zones

A fifth component, MIKE 11 sediment transport, will be incorporated in a further development of the model (see Appendix 3).

Before developing a numerical model it is first essential to obtain a conceptual understanding of processes driving the delta hydrological system. Secondly, development of a strategy based on project priorities is important to guide the process.

4. APPROACH AND CONCEPT

4.1 Approach

The approach to the development of an integrated hydrologic model depends on the conceptual understanding of the Delta hydrology. Data collected and interpreted as part of a large number of scientific projects in the delta form the basis for the conceptual model. Several authors have contributed to the general description of Delta hydrology including large scale Delta wide studies and localised projects describing the more detailed hydrological responses.

The Okavango Delta is the largest inland delta in the world and constitutes a vast and unique wetland system. The basis for the Delta is the abundance of water distributed over a 4,000-15,000km^2 flooded area (depending on year and season) surrounded by the semi-arid Kalahari Desert.

Water forms the fundamental physical basis for the entire ecosystem. Any management and protection plan must thus first and foremost aim at preserving the hydrologic regime, while facing challenges in terms of linking hydrology and ecosystem responses. Bearing in mind that the natural climatic conditions of the Okavango Delta and the upstream catchments are highly variable in both the short and long terms, the impacts of water development or future changes in eg climate should be evaluated by their impact on the Delta hydrology. Impact assessments rely on estimates or tools capable of addressing the complexity of cohesive hydrologic processes.

The hydrology of the Okavango Delta is complex, dynamic and in many respects unlike most other river catchments. Some striking characteristics include:

- The Okavango River system does not discharge to the sea or a lake but spills across the Okavango Delta
- Insignificant downstream discharges (on average 1% of inflows) due to high losses
- River channel network with numerous splits and bifurcations
- Rainfall is of relatively lesser importance than inflows with respect to maintaining flooded areas (a large proportion of total rainfall input to the Delta is lost by evapotranspiration on dry land areas and does consequently not add to the water levels in flooded areas)
- Highly dynamic flow and flood conditions (from year to year)
- Slowly propagating flood wave due to low gradient and vegetated flow paths
- Irregular spatial and temporal recharge of the ground water aquifer by flood water
- Large hydrologic contrasts among permanently flooded areas, temporarily flooded areas and dry land extending towards the surrounding Kalahari desert

The Okavango Delta includes the upstream Panhandle, a proximal alluvial fan in the central part and a distal fan section towards the downstream perimeter. Runoff from the upstream catchments of the Cuito and Cubango Rivers in Angola enters the northern part of the Panhandle through the Okavango River. The Panhandle forms a corridor confined by fault lines. The Okavango River meanders through the low lying

area (Figure 4.1) and expands beyond the narrow main channel to flood the major part of the Panhandle.

An abrupt expansion downstream of the Panhandle to a vast low relief, alluvial fan causes the river to spill across large flood plain areas (Figure 4.2) and split into separate channel systems. Three main rivers are formed, namely: Thaoge towards the south west, Jao-Boro to the south and Maunachira-Khwai to the east. Further downstream additional bifurcations split the channels into a large number of smaller flow paths which again join to form a complex flow system of flood plains, flow splits and confluences.

The channels are subject to partial blockages by vegetation (Figure 4.3) forcing the water on to wide flood plains. Due to limited conveyance capacity, the river branches spill to adjacent flood plains and generally the flow takes place as a combination of river and overland flow with multiple points of flow exchange between the river and the flooded areas. Permanently flooded areas cover approximately 4,000km^2 at low flow while temporarily flooded areas may cover two to three times the permanently flooded area depending on the magnitude of the inflows.

Figure 4.1: Okavango River Meandering through Panhandle

The total rainfall volume (approximately 480mm/year) on the delta corresponds to approximately half the total volume entering the flooded areas. Due to the low topographic gradient and high rates of evapotranspiration, the redistribution of water internally in the delta by runoff is limited. Locally the runoff from rainfall may flow to depressions, but generally rainfall outside the flooded areas only adds temporarily to subsurface storage before being lost to evapotranspiration.

As the flooded area expands infiltration accounts for significant losses. The sandy soils have relatively high infiltration rates. The unsaturated zone becomes saturated and the ground water levels approach flood water levels. In contrast to the rapid and full recharge by flood water in flooded areas, the recharge by rainfall in dry land areas is very limited. In temporarily flooded areas the recharge is closely connected to flood water levels along the channels and flood plains. Considerable variation in the annual flood extent implies highly variable aquifer recharge. In distal fan areas a highly irregular freshwater aquifer is observed and confined pockets of fresh water along channels may only be recharged during high flood years.

Figure 4.2: Flood Plains of Proximal Fan Zone

Rainfall occurs in the months of October to April while the river peak discharge upstream in the Panhandle occurs around April. Due to a slowly propagating flood wave the maximum flood conditions occur around July. Downstream flow peaks indicate a total travel time through the delta of around four months.

The balance between rainfall and inflows on one hand and losses including evapotranspiration and subsurface storage changes on the other controls the annual flood extent of the delta. In addition, analysis of inflows and flood areas suggests that the previous year's flood extent and recharge influences the flooding /3/.

Increasing surface water area gives rise to increased evaporation. The potential rate of evapotranspiration exceeds 6mm/day (2,190mm/year). The actual rate of evapotranspiration, however, varies from zero in dried out soils at the perimeter of the delta.

Vegetation plays an important role in the annual cycle of transpiring water in the soil and upper aquifer system. Local water level gradients induced by significant transpiration losses may even locally drive ground water flows during low flood periods. Vegetation in the delta is closely interlinked with the flood regimes. The availability of water is the main controlling parameter on vegetation distribution and, due to blockages formed by dense wetland vegetation such as papyrus (/11/), the actual distribution of flood water depends on the vegetation. Both dense wetland vegetation and dry grasslands are common in the delta with transition zones in occasionally flooded areas. On the bushland and grassland areas scattered trees have developed deep root systems (10-20m) to extract ground water for transpiration during prolonged drought periods. Distribution of vegetation type responds to changes in flooding from eg climatic variations within a relatively short time period, a single or a few wet years.

Along shorelines of Delta islands, the salinity of the soil affects the distribution of vegetation types. Island interiors are often barren due to high salinity. Vegetation with high salinity and drought tolerance occupies an intermediate zone and finally

wetland species are found in close proximity to the frequently flooded areas. On the smaller scale, salt concentrations thus influence actual evapotranspiration rates.

Considerable scientific work has been carried out with respect to the Okavango Delta hydrology. To understand the overall driving hydrologic, hydrogeologic, morphologic and climatic driving forces it is important to understand both the local scale and the large scale. Several field studies have been dedicated to describing local flow phenomena. In contrast the use of remote sensing data has allowed large scale analysis, eg /3/.

Figure 4.3: Encroaching Papyrus

The work within different fields has added to the understanding of delta hydrology, but no attempts have been made to include collectively all relevant processes in one quantitative and physically based tool. The ODMP hydrologic model includes more relevant surface and subsurface processes and their interaction than any previous model approaches, and provides a broader and more robust modelling framework to quantitatively describe the delta hydrology.

4.2 Conceptual Hydrologic Model

4.2.1 Surface Water

The Okavango Delta surface water system comprises a mosaic of permanent wetlands and temporarily flooded areas partially connected by a river and stream network. The distribution of water, flows and water levels depend on the river network layout, channel conveyance capacity, topography, vegetation, surface–ground water interaction and evapotranspiration losses.

Water distribution by channel flow requires a representation of all major river branches affecting the larger scale flow pattern. Apart from actual upstream–downstream water level gradients, channel conveyance depends mainly on bed slope, width of river and resistance to flow. Water levels in high resistance reaches with a low bed slope build up and, due to backwater effects, spills are induced along upstream river segments. Topography affects the distribution of flood water, which again impacts river conveyance and water levels. This is most prominently observed

in the lower part of the Panhandle and the upper expanding alluvial fan, but applies to the channels in the flooded areas in general.

As water levels rise in the rivers, water moves on to the flood plains. Initially the wave propagates to areas immediately adjacent to the channels and then slowly propagates across the wide flood plains filling up back swamps and lagoons (Figure 4.4). Due to the significant flow across flood plains both along and away from the main channels, and the travel time in local channels, flood plains and pool flow rates and directions in individual sections of the delta are distinctively time varying. For example in the early flood stages the filling up of water bodies may cause several shifts in flow, but the seasonal rise and fall of water levels in main rivers drive the overall flow distribution.

Figure 4.4: Channel and Flood Plains of Upper Khwai River

4.2.2 Subsurface Flows

The subsurface waters are a primary hydrologic component of the Okavango Delta. They play an important role in relation to surface water losses in the early flood stages, thus restricting the total area of flooding. Relatively small subsurface deficits due to high floods the previous years may effectively lead to higher flood extents in years of low inflows.

Infiltration rates are generally high in the sandy soils of the Okavango Delta. Unless continuously supplemented by flood water from the surface, the unsaturated soil column quickly drains. The unsaturated zone does not to any significant extent impede the ground water–flood water interaction.

Different views of delta ground water flows presented in the literature include a regional, horizontal aquifer flowing across the delta as opposed to a local conceptual model of groundwater dynamics, suggesting insignificant ground water flow rates apart from local adjustments to ET losses and annual recharge in flood plains. According to the regional view, ground water would flow across the downstream Thamalakane fault line and potentially into the surrounding Kalahari along the eastern

and western perimeter. Isotope contents of ground water samples and ground water model tests do, however, indicate that there is little or no ground water flowing from the delta to the surrounding areas /9/.

Independent ground water modelling tests performed by the DWA Modelling Unit support the fact that local water level gradients determine ground water flow directions rather than regional gradients. Consequently, the role of ground water should be understood at a local scale where vertical fluctuations in ground water tables in response to flood water levels and ET losses are of the essence.

Measured time series of water levels in observation wells across island transects of the temporarily flooded delta show that ground water levels quickly rise, reaching surface water levels in the early flood season. The ground water table decreases from flooded areas towards dry island interiors where vegetation rooting depth determines the minimum water level. Transpiration by the vegetation controls the water level below dry islands and, due to the induced water level gradient, flood water continuously recharges the ground water and replenishes root zone deficits in riparian fringes. In effect transpiration from ground water in vegetated belts along the island perimeter maintains local ground water flow and accounts for an important loss term in the water balance. (Figure 4.5 shows scattered islands and flooding in the delta.)

The reasoning implies that attention should primarily be directed towards near surface-ground water fluctuations during annual changes in flood levels, and to a lesser extent the deep aquifer conditions.

In addition, geophysical surveys in potential well field areas along the downstream Boro River /5/ clearly show an irregular pattern of fresh water lenses embedded in saline ground water. Significant recharge of ground water takes place only along surface water flow paths depending on the frequency of flooding, whereas recharge by rainfall is very limited. A continuous fresh water aquifer is only found in the permanently flooded areas of the delta. In the dry land areas close to the delta perimeter recharge rates approach those of the adjacent Kalahari Desert. This does not support any significant or continuous ground water flow.

Ground water abstractions in villages along the western perimeter of the delta and for the water supply to Maun may locally cause drawdown of ground water tables. At the larger scale the abstractions will not affect delta flood extents or discharges but merely lead to mining of the local fresh ground water body.

4.2.3 Evapotranspiration

Evapotranspiration (ET) is the dominant loss factor in the Okavango Delta water balance. Compared to total inflows only about 1% is discharged to the downstream outflows. The annual potential evapotranspiration rate exceeds the rainfall, and the permanent flooded areas can only be sustained by a significant supplement of flood water. In the dry land areas scattered flooding in local depressions occurs in response to high intensity rainfall, but infiltration losses and in particular ET losses quickly dry out local ponds.

The actual rate of evapotranspiration is highly variable between flooded and dry land areas, which is key with respect to quantitatively describing the total delta ET losses. In dry land areas with sparse or withered vegetation, soil evaporation may be the dominant ET loss factor along with limited transpiration by the vegetation. After longer dry periods the soil is effectively dried and evapotranspiration ceases at residual water contents of the soil matrix. If, on the other hand, sufficient water is available on the surface and in the soil, actual ET rates may reach the potential rate of approximately 2,200mm/year. Expanding and retreating floods control significant

temporal changes in actual rates of ET, and ET losses are a main controlling factor in containing the flood plain extents.

Figure 4.5: Scattered Islands and Flooding affecting Ground Water Recharge Patterns

Looking at local evapotranspiration dynamics, the role of salinity in the soil and ground water also plays a role. This is typically visualised by island transects. In combination with flood water levels, topography and the ability of the vegetation to extract ground water from the aquifer salinity may act as an controlling parameters. The elimination of salinity sensitive plant species affects transpiration rates and possibly the total water losses.

ET terms including transpiration by the vegetation, evaporation from free water surfaces and soil evaporation must be computed throughout the delta, but their relative importance depends strictly on local conditions such as simulated flood depth, soil water content, etc.

The dynamic flood conditions must be incorporated in computations of distributed and time varying ET rates:

- Transpiration of the vegetation as a function of actual soil moisture content, eg during saturation of the soil profile by infiltrating flood water, or depletion of water in the soil profile during continued depletion by ET losses
- Evaporation from a free water surface for periods of flooding or local ponding as a function of main driving climatic factors such as wind speed, air temperature, humidity, etc
- Soil evaporation enabling ET losses for dry land conditions.

Effects of salinity are seen across the Delta at the local scale. It is, however, most visible in Delta islands where the availability of water may be a major limiting factor on vegetation cover. The more detailed description of short term and long term processes relating to salt, water, soil and plant interaction on both the large and small scales is complex. Water quality effects on the Delta hydrology and water balance

have not been included in the conceptual model and the subsequent numerical model.

On the larger scale the actual rates of evapotranspiration are affected by the density of the vegetation cover, which again reflects the availability of water expressed through depth to the ground water table or flood water levels, flood duration and flood frequency. Evapotranspiration rates should thus be a function of vegetation characteristics and actual water levels (soil water content), or alternatively simply related to water levels assuming that vegetation will quickly adapt to changes in the flood regime. Here the first option has been chosen.

4.3 Key Hydrologic Processes

The following hydrologic processes of the Okavango Delta are identified as important with respect to firstly the conceptual description and secondly implementation in a numerical model:

1. Water distribution by channel flow
2. Channel–flood plain flow interaction
3. Water distribution by overland flow during expansion and retreat of floods
4. Infiltration of rainfall or flood water through the soil and unsaturated zone storage changes
5. Ground water recharge, flow and storage changes
6. Dynamic ground–surface water flow exchange
7. Flow and water distribution from rainfall
8. Evaporation from free water surfaces of permanent and temporary flooded areas
9. Transpiration from the vegetation
10. Soil evaporation in dry areas.

To include the above processes in a numerical model a suitable modelling tool must be chosen. The integrated nature of the Okavango Delta hydrology does not favour ground water models with adaptations to account surface water flows through simplified boundaries. River hydraulic models may be developed to describe the channel and flood plain flows, but lack the ability to include distributed hydrologic processes accounting for ET and subsurface losses. The only consistent modelling approach must be based on dynamic, distributed and integrated models with emphasis on the entire hydrologic system, as individual components of the hydrologic cycle cannot be separated.

On the other hand, the complexity of the Okavango Delta hydrology exceeds the data available to provide a detailed account of all processes. Despite emphasising the need for an integrated model, it is recommended to consider the simplest description possible for the various processes, avoiding excessive data requirements.

The combined MIKE SHE (/12/) and MIKE 11 (/14/) system is the only known, well tested Integrated Hydrologic Modelling system with a full representation of both the surface water and the subsurface regime. The ODMP hydrologic model development must, however, honour the conceptual model, which implies that the MIKE SHE and MIKE 11 modelling systems are adapted to the delta hydrologic conditions by choosing among the different solution methods.

5. INTEGRATED HYDROLOGIC MODEL

5.1 Components

To implement the conceptual processes outlined in an Integrated Hydrologic Model the following MIKE SHE and MIKE11 components are selected:

MIKE11 HD: River hydrodynamic model solving the Saint-Venant equations in a 1-D river network. MIKE11 computes water levels and discharges throughout the major river branches of the delta. Water in the river network is subject to flow exchange with ground water by leakage and with the flood plains by spills or return flows.

MIKE SHE OL : Describes overland flow by solving the Saint-Venant equations in a 2-D representation of flooded areas including flood plains. MIKE SHE OL simulates water levels and flows in all temporarily or permanently inundated areas. Overland water is subject to dynamic exchanges with the river module (MIKE 11), with the unsaturated zone by infiltration and with the SVAT module in terms of ET losses

MIKE SHE SZ : Saturated zone flow (ground water) is described by the Boussinesq equation (2-D or 3-D) with ground water levels and flows as the main variables. MIKE SHE SZ is dynamically linked with the river and overland components by leakage and with the unsaturated zone through recharge. In addition water may be lost directly from the ground water by ET losses (MIKE SHE SVAT)

MIKE SHE UZ: Unsaturated zone flow is described by a 1-D approximation of the Richardson's equation where capillary forces have been ignored (due to generally medium textured sandy soils throughout the delta). MIKE SHE UZ is connected to the overland component and infiltration is simulated depending on actual flood water depth or in dry areas solely from rainfall. When infiltration from flood water has raised ground water levels above ground level, MIKE SHE UZ is left out of the simulation and is only re-activated in the integrated model when unsaturated conditions recur. Within the root zone ET losses may reduce the unsaturated zone soil water content due to soil evaporation or transpiration by vegetation. At the dynamic interface between the unsaturated zone and the ground water, exchange of flow occurs as percolating water recharges the aquifer.

MIKE SHE SVAT: A Surface-Vegetation-Atmosphere Transfer module is applied with the objective of simulating distributed and time varying potential ET losses in the ODMP hydrologic model. The SVAT module simulates heat fluxes between the soil and vegetation layers including exchanges with the atmosphere. A number of resistances is applied to control energy fluxes. The module is driven by meteorological inputs and includes a number of vegetation parameters. Most prominently the SVAT module provides ET losses in time and space affecting the hydrologic cycle. ET losses are split into soil evaporation, transpiration and evaporation from inundated areas. The SVAT module is dynamically linked to MIKE SHE UZ, MIKE SHE SZ and MIKE SHE OL, and water is lost from the respective hydrologic components due to evapotranspiration.

All of the above model components are integrated through dynamic flow couplings and total water balance data from the delta are produced (Figure 5.1).

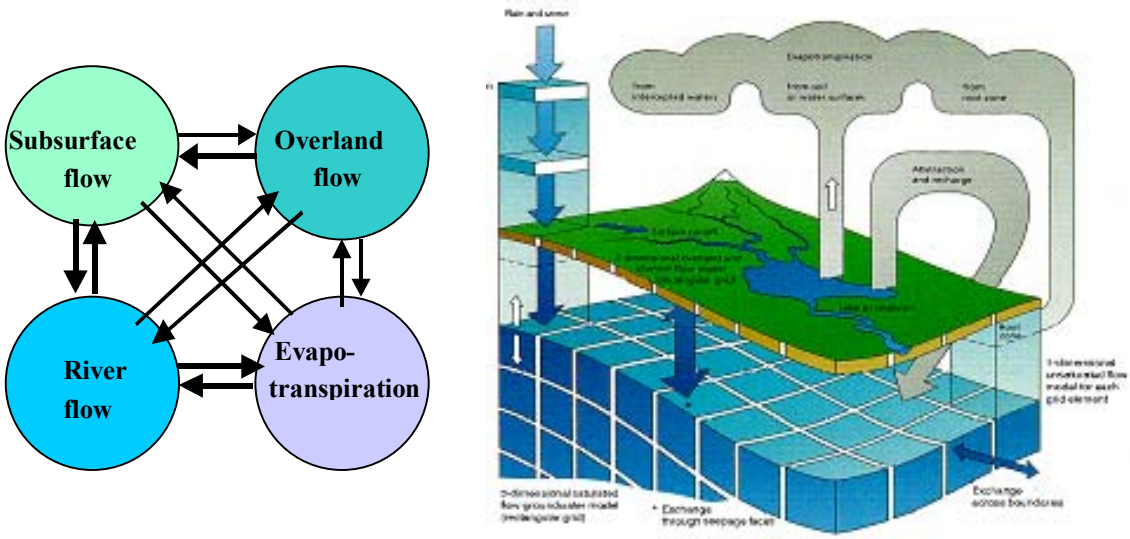

Figure 5.1: MIKE SHE Hydrologic Modelling System and Couplings

5.2 Model Area

The horizontal extent of the Okavango Delta Integrated Hydrologic Model has been specified considering:

(1) Sufficient to cover the area of interest in the current project

(2) Hydrologic boundaries defined by fault lines and topography

(3) Model simulation run times

(4) The largely separate hydrologic regimes of the delta and the surrounding Kalahari Desert.

The model area covers 28,782km^2 from the upper Panhandle at Mohembo to the downstream Thamalakane and Kunyere faults, including the upper part of the Boteti River and Lake Ngami to the south west (Figure 5.2).

5.3 Spatial Scales

A uniform computational finite difference grid is used. The choice of grid resolution determines the detail of the model outputs. Input data at a finer resolution (eg topography) will be aggregated to the grid size. Furthermore the grid resolution affects the total number of computational elements to be solved during individual time steps of the simulation.

A 1km by 1km grid is adopted, which implies that:

(1) Model input data at a finer spatial resolution will be aggregated or interpolated in the computations

(2) The model simulates responses in 1km^2 grid elements and does not explicitly sub-scale variations

(3) The detail of model outputs is dictated by the choice of grid resolution. Model results will not support analysis at a finer spatial detail.

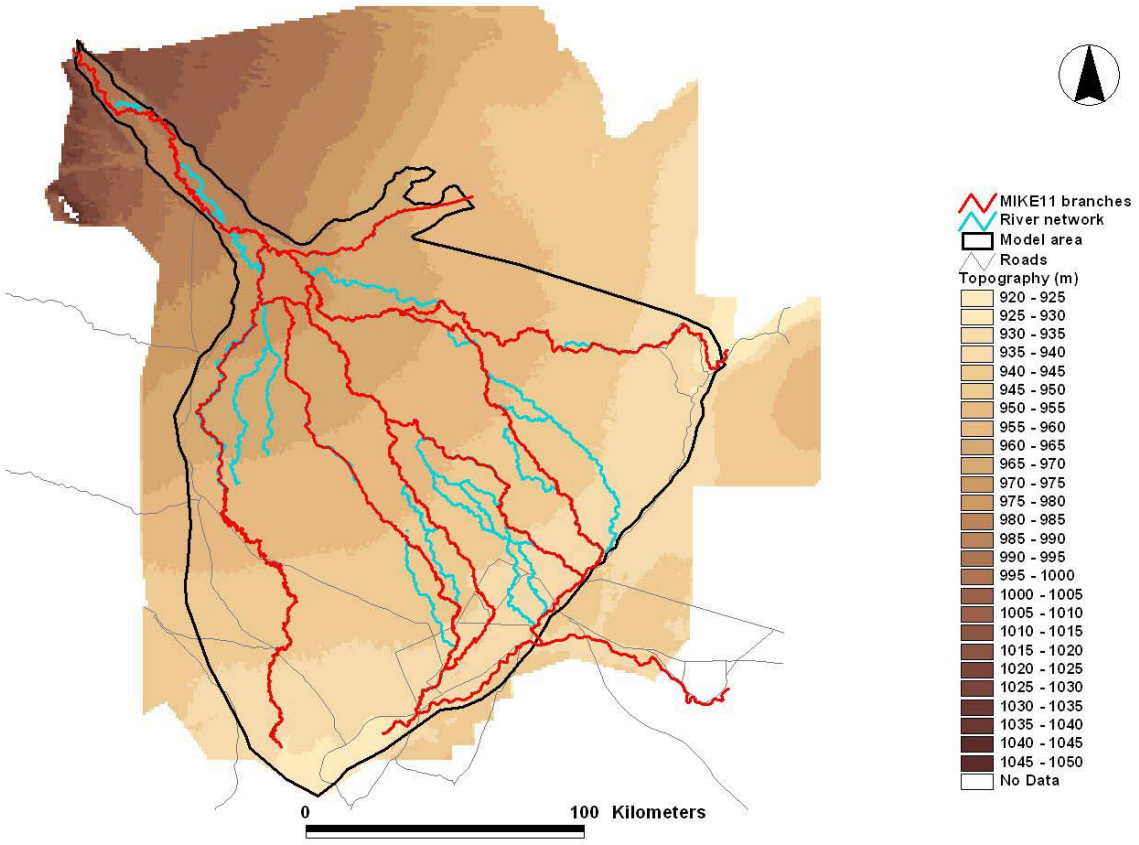

Figure 5.2: Model Area

The MIKE SHE–MIKE 11 modelling system allows for a more detailed model approach addressing localised issues by carrying boundary conditions from the larger scale model to a local scale model. This is, however, not within the scope of the ODMP, which addresses the entire Okavango Delta hydrology. Apart from any run time model limitations in pursuing a finer spatial scale, the reliability of model simulation results will depend on the density of the underlying input data.

5.4 Temporal Scales

The time scales of for example surface water and ground water are different. Surface water flows respond relatively quickly to changes in eg rainfall whereas aquifer flow in response to rainfall and subsequent recharge is likely to occur at a much slower rate. This is taken into account by assigning appropriate simulation time steps for the individual hydrologic components. The smallest time step is applied in the river network model (5 minutes) and the largest in the ground water (48 hours). To avoid numerical instability in the surface water module during periods of extensive flood spills, a 4 hour time step is used in the overland flow solution. The ET component runs in 4 hour time steps, which is considered the largest allowable time step if diurnal variations in solar radiation and ET rates are to be captured by the simulation model.

More importantly, when extracting model results for further analysis, is the storing frequency. Typically the results are stored at a frequency supporting the actual use and preventing excessive result file sizes and post-processing. Surface water results

are stored as hourly or daily values, while ground water results are stored once every 1 to 3 months in model production runs.

The MIKE SHE model has automatic time step control. When significant changes in for example rainfall occur, the time step is automatically reduced. After reduction the time step will gradually be increased until it reaches the maximum value specified by the user.

5.5 Surface Water

5.5.1 Introduction

Surface water comprises both river channel flow (1-D), overland flow (2-D) and their distributed, dynamic interaction. The surface water component of the Integrated Hydrologic Model is subdivided into MIKE 11, with a full hydrodynamic description of the flow through the river network, and MIKE SHE OL for simulation of overland flow (flood plain flow), using the diffusive wave approximation. The coupling between the river and overland model is essential in simulating the extensive river-overland spills and overland-river drainage.

5.5.2 River Flow Model

Network

The surface water flow through the delta is concentrated in a complex network of river channels which distribute the flow through the delta and over the flood plains and swamps. The distributed component of the hydrologic model has a spatial resolution of a one kilometre grid. The river channels are 5 to 100m wide and are thus too fine to be resolved by the 1km grid applied for the distributed hydrologic model. To include both channel flow and flood plain flow at the appropriate spatial and temporal scale two numerical solvers run in parallel with a dynamic coupling allowing water to be exchanged through simulation of spills.

A detailed network of river channels has been built up from the intimate knowledge of DWA staff of the delta, from previous researches particularly those based at Witwatersrand University, and from the 2002 aerial survey of Botswana conducted by the Department of Surveys and Mapping. From this, a simplified network has been set up, based on the conveyance of the channels including poorly defined channels better described as overland flow paths (eg the Matsebe), transverse spatial distribution, availability of cross section data and location of gauging stations. The detailed and simplified networks are shown in Figure 5.3.

The river channels are represented explicitly in the Integrated Hydrologic Model by the one dimensional hydrodynamic component. The hydrodynamic component covers the river channel, plus a one kilometre flood plain on each bank, with a total width around 2km. The hydrodynamic component was initially set up with the river cross sections extending over the entire surface area of the delta (figure 5.4). For incorporation into the integrated model, these sections are constrained to a 2km width, the flood plain overland flow being handled by the distributed (one kilometre grid) component.

The flow through the river channels is automatically coupled to the one kilometre distributed overland flow component. Evapotranspiration to the atmosphere and infiltration to ground water from the river channels is simulated within the domain of the distributed hydrologic model, though not where the river channel extends beyond this, ie for the lower reach of the Boteti River.

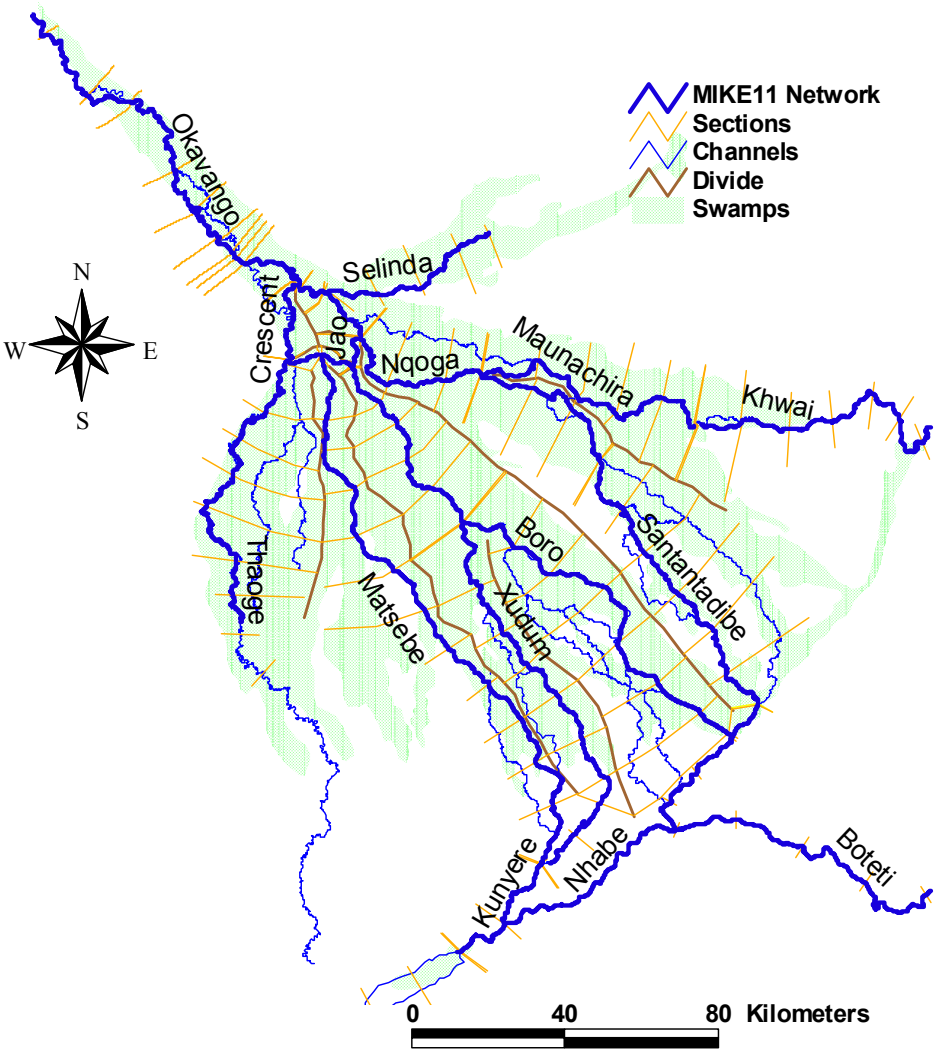

Figure 5.3: River Network represented in MIKE 11 Model

Cross Sections

The river channels are defined by sections at gauging stations surveyed by DWA, researchers and the topographic model (see Figure 5.4). Initially only the gauging station at Mohembo was connected to the national datum. In the course of 2003/04, DWA commissioned DSM to level all the water level gauge bench marks using high accuracy DGPS, giving centimetre accuracy.

The cross section database for the hydrodynamic model has been built up using the surveyed cross sections, interpolating between these sections, and where not otherwise available estimating absolute levels (relative to the national datum) in relation to the topographic model. Cross sections for reaches better described as flow paths rather than defined river channels have been taken from the topographic model.

The modelling system allows direct extraction of sections from the topographic model into the database, within ArcView. The surveyed channel sections have been incorporated into the sections extracted from the topographic model (see Figure 5.5). For integration with the distributed component, the sections are constrained to a total width of 2km.

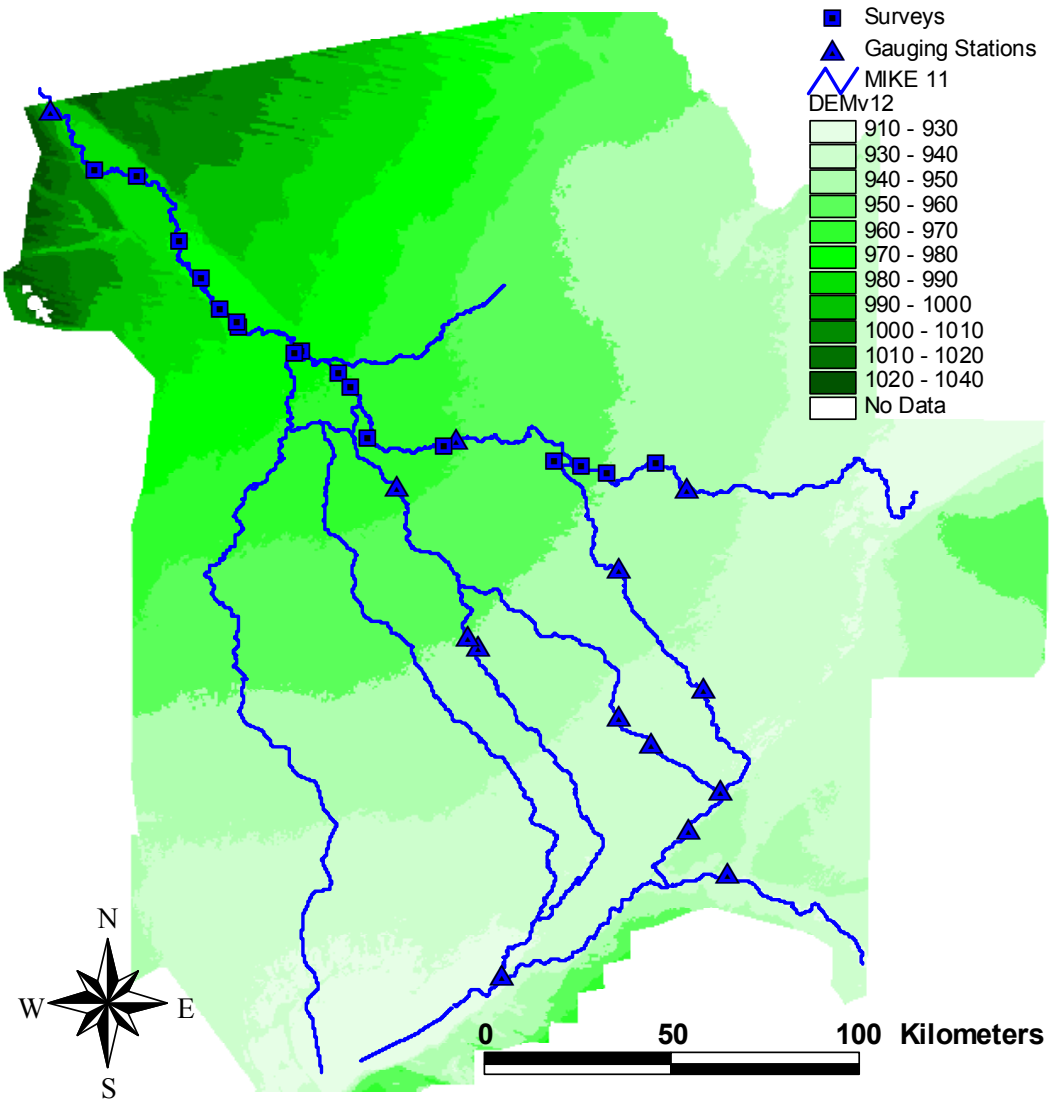

Figure 5.4: Surveyed and Gauging Station Cross Sections

Resistance to Flow

The resistance to flow through the river channels is described in four ways:

(1) A single global parameter (optionally Manning or Chezy).

(2) An assigned resistance for selected river reaches, overriding the global parameter.

(3) A factor relative to the depth of flow.

(4) A factor applied in relation to the distance across the section.

A global value of the Manning resistance factor M of 20 is applied, reflecting the general level of bed and form resistance, channel vegetation and sinuosity. This is varied along the reach, reflecting the general density of the vegetation.

The factor is further varied in respect of the depth of flow, thus a high resistance for low flows in drying channels, reflecting small scale bed topography not captured by the surveyed sections. Finally, the resistance factor is varied across the section width, reflecting the clear flow of the open channel, and the high resistance from vegetation on the lateral flood plains. Channels blocked by vegetation have a high flow resistance, similar to that of the flood plains.

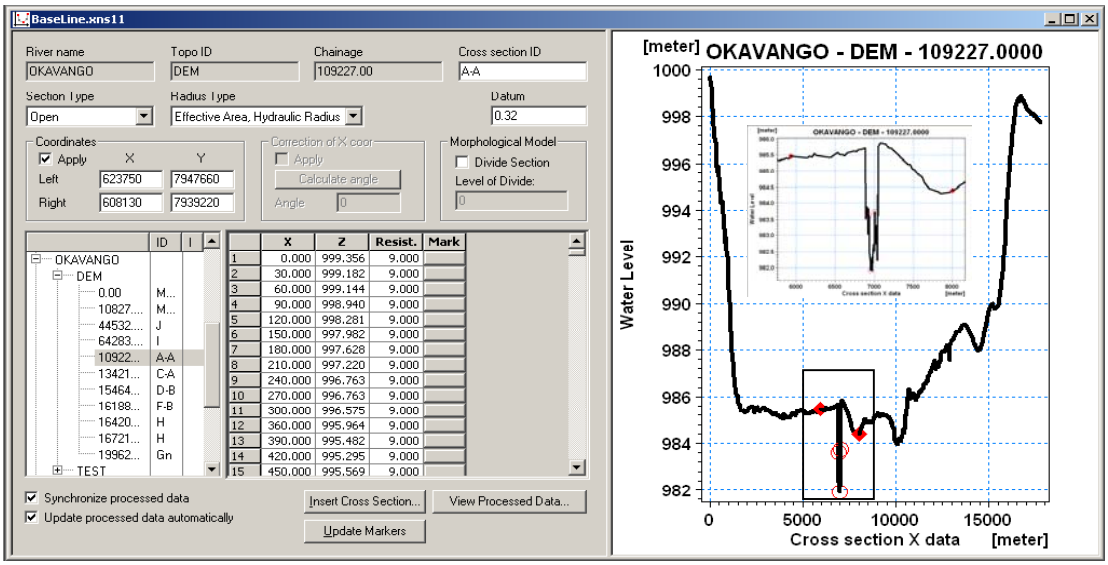

Figure 5.5: Cross Section Database

The facility exists to vary the resistance with time, as it may vary with the season and state of flow, low as high flood flows clear channels, and high in the dry period as dying vegetation blocks flows. This has not been applied at this stage in the model development.

Boundaries

The surface and ground water system in the distributed component of the hydrologic model is closed, ie there is no flow entering or leaving the system. The flow into and out of the delta is described by:

(1) In the hydrodynamic surface water component, the river channel inflow at the upstream extent of the model on the Okavango River, presently the international border with Namibia, and the outflows from the four river channels: the Thaoge, the Boteti, the Khwai and the Selinda.

(2) In the distributed component, the loss to the atmosphere is computed by the MIKE SHE ET component (see section 5.8).

The upstream inflow boundary is taken as the daily flow record from the Mukwe water level gauge (approximately 45km upstream of the border), with the rating curve derived from the gauged flows at Divundu (30km upstream). This flow hydrograph will be slightly attenuated as the flood wave propagates through the river channel to the border downstream. This minor difference is considered preferable to using the flow record at Mohembo where a significant proportion of the high flows bypass the station over the extensive flood plain on the left bank. If cross sections referenced to the regional datum become available, the model can be extended upstream to Divundu.

The outflow conditions on each river channel are described by a low weir, a few centimetres above the bed. This retains a negligible amount of water in the channel upstream, but aids stability of the outflow.

5.5.3 Overland Flow Module

The overland flow module simulates overland flow driven by water level gradients. Gravitation and friction forces are considered in a diffusive wave approximation of the Saint-Venant equations.

Surface topography is the single most important input with respect to overland flow. The ODMP Topographic Model /1/, (version 12.1), has been used as input to the ODMP hydrological model. The topographic model covers the entire model area. The topographic model has been produced at a 30m grid resolution. The hydrologic model applies a coarser computational grid than the topographic model and consequently the 30m model has been converted to a 1km grid by interpolation using ArcView Spatial Analyst.

The dependency of overland flow results on accurate topographic model input can be illustrated for two cases. In the Panhandle the river water levels are significantly above the river cross sections and water spills on to wide flood plains. A local elevation difference between the channel cross sections and the adjacent flood plain determines where spills predominantly occur. In addition, flow direction and storage changes in the flood plains are closely connected with the underlying topographic model, ie absolute surface elevations.

Downstream, in the extensive flood plains of for example the Jao-Boro and Maunachira-Khwai systems, the simulated water levels and extent of flooding are dependent on the topographic gradients where relatively small changes in slope may have pronounced effects on simulated flow patterns and flow rates. Due to limited penetration depth of the radar used in deriving surface elevations, the uncertainty of the topographic model is higher in the deeply flooded areas than the remaining part of the delta. If elevations are over-estimated this will imply shallower flooding and potential underestimation of storage.

The overland flow direction is determined by the water level gradients but the flow rates also depend on the surface roughness. Manning numbers are used as model input to assign distributed surface roughness. Overland surface roughness is not easily measured and no data specific for the delta have been found. The resistance to flow is, however, mainly correlated with the vegetation and subscale topographical variation. Vegetation in the permanently flooded areas is dominated by papyrus over large areas. The papyrus is very dense with an extensive root system (rhizomes) effectively reducing the cross section flow area and providing high resistance to flow. Less frequently flooded areas are characterised by scattered bush and grass with less resistance to flow.

A close inspection of recent vegetation maps (S Ringrose, HOORC) shows a high degree of correlation with flood frequency maps suggesting that vegetation types depend on flood regime and that vegetation is a controlling factor in the extent of flooding. Consequently the surface roughness has been distributed according to the vegetation types. Three zones representing wetland vegetation, riparian vegetation and bush-grass land areas have been used. It is likely that variable roughness conditions occur within these three broad classes, but since field data do not exist to support a more detailed distribution, the number of sub-divisions has been restricted. The absolute roughness coefficients applied for the vegetation zones (Manning numbers) are subject to calibration while maintaining a fixed ratio reflecting generally higher resistance in densely vegetated areas.

5.5.4 River–Overland Flow Coupling

The river network–flood plain flow coupling has been built on an existing dynamic flow exchange description in MIKE SHE–MIKE 11. The 2-D MIKE SHE overland module

simulates 2-D flow and water levels in all areas of the model (if there at any point in time is water on the surface). The MIKE 11 river hydrodynamic module simulates the channel flow (Q) and water levels (H) by an alternating grid node system. At any simulation time step water may be exchanged between the MIKE 11 network H-points and the closest assigned grid element (flood code grid cells) along the river branches, provided that a water level difference exists to drive the flow /12/.

Flood codes have been specified in all river branches where flooding might occur excluding the far downstream river reaches. Spills from the river on to the flood plain and drainage from the flood plain to the river branches occur as a function of water level gradients. When river water levels rise above the water level of the adjacent flood code grid cell, eg in the early stages of the flood season, a river water volume is moved from the 1-D river to the flood code cell and it becomes subject to 2-D horizontal distribution of eg a flood wave across the flood plain. At retreating flood water levels of the river, the flow is typically reversed but, in the fully distributed model, direction and magnitude of water level gradients may vary depending on the progress of the flood wave, the gradual process of flooding and drying flood plains, ET losses and other hydrological processes affecting the actual simulated water level in both the river network and on the flood plains. The river and flood plain resistances effectively control primary river reaches for exchange of flow.

Initial model runs revealed a few cases of significant flood spills and subsequent flooding in areas where little flooding occurs according to satellite images. In most cases river water is spilled on one side of the river depending on river bank levels and local flood plain topography. Field data and remote sensing data suggest spill predominantly occurs on the other side in some cases. Due to lack of detailed cross section data, uncertainties in the topographic model and the effects of variation in local vegetation cover, it is not possible to simulate such local details, but they may affect downstream flooding patterns. The relative proportion of spills on each side of the river can be controlled in the model only by adjustment of the flood codes favouring spills to a particular side of the river branch. For example, in the upper Nqoga flood codes have been adjusted to obtain a better simulation of river spills on to the adjacent flood plains.

In addition to the river–flood plain exchange, the integrated model features a ground water–river flow exchange mechanism. Based on local actual water level gradients between the river and the adjacent aquifer, leakage losses from the river or ground water discharges to the river (baseflow) are simulated. Losses through the river bed may be insignificant in permanently flooded areas with insignificant water level gradients, but in the downstream dry land areas of the delta water is lost. Due to the sandy aquifer and low content of sediment, the river lining is not assumed to represent any significant resistance to flow. The ‘full hydraulic contact’ option of the model has been used for all river branches.

5.6 Unsaturated Zone

The unsaturated zone model of MIKE SHE simulates time-varying vertical flow and storage in characteristic soil columns. A number of characteristic soils is identified and hydraulic parameters in terms of hydraulic conductivity curves and retention curves are specified as model input. A number of alternative unsaturated zone solution methods is available in MIKE SHE. Given the relatively coarse texture of the fine to medium sands of the delta, it is reasonable to assume that capillary forces are negligible. Consequently the ‘Gravity flow’ solution scheme is chosen as opposed to the ‘Full Richardson solution’ option. The benefits of the ‘Gravity Flow’ option include shorter simulation run times and reduced soil data input (retention curve data not used). Flow against gravity may occur locally in the Delta but it is mainly a function of

water uptake by plant roots and not the capillary potential of the soil. The soil samples collected across the Delta did not include soils of high organic content. Peat deposits may locally affect the water movement from the ground water table to the root zone.

A soil map is applied to distribute characteristic soil columns representing the dominant soil types. A GIS based soil map from the Botswana Agricultural Ministry was used to classify the delta soils (Figure 5.6). Largely the finer sediments are deposited close to the flow paths and the coarser materials are found in dry land areas. The general picture is, however, disturbed by apparent discrepancies where separate maps have been merged to cover the entire delta. The saturated hydraulic conductivities of the soil control infiltration rates are shown in Table 5.1. The range of conductivities is narrow suggesting a relatively homogeneous topsoil in terms of hydraulic properties. Infiltration rates are primarily determined by flooding or high intensity rainfall while soil infiltration capacity only causes a slight delay in subsurface response to flooding.

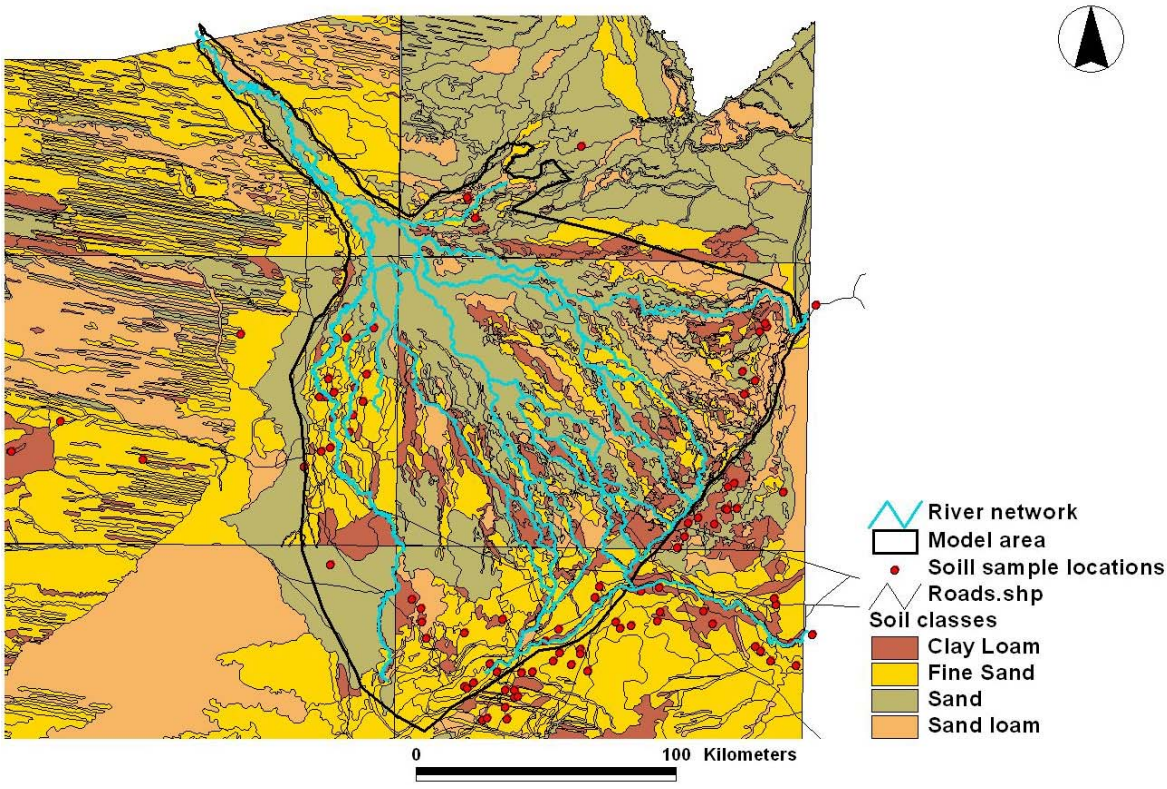

Figure 5.6: Soil Map Classification

Table 5.1: Delta Soil Classes and Associated Hydraulic Parameters

Soil ID	Soil Sample ID	Saturated Hydraulic Conductivity (m/s)
Clay loam	TO700_346	5.3e-006
Fine Sand	GO0309_83	7.6e-006
Sand	MA0433_165	6.3e-005
Sand loam	TO0891_372	5.8e-006

In the numerical model the vertical soil columns are discretised (subdivided) into 0.1-0.5m computational elements for solving the unsaturated flow equations.

5.7 Ground Water

The unsaturated zone extends by definition from the soil surface to the ground water table. Since a dynamic ground water is required to simulate the subsurface storage changes during expanding and retreating floods the thickness of the unsaturated zone itself becomes time varying as well. In permanently flooded areas the unsaturated zone is completely ignored as saturated conditions prevail. In the temporarily flooded areas the unsaturated zone varies in response to the flood dynamics and is ignored for longer periods of flooding. In the dry land areas the ground water table fluctuations are much less and the depth of the unsaturated zone is almost constant. Due to low infiltration rates in the dry land areas very limited unsaturated flow occurs. During rainfall events water infiltrates through the top soil but recharge to the ground water may not occur due to water deficits in the soil and high rates of evapotranspiration. Water stored in the soil matrix when the water content falls below field capacity may be subject to soil evaporation.

The ground water component of the ODMP hydrologic model mainly serves to account for storage changes following the flood expansion and flood retreat. In accordance with the conceptual understanding of ground water, the regional deep aquifer ground water flow is negligible as local gradients towards depressions are stronger than the gradients across the delta. It is the aim to include the effect of ground water on the surface water system rather than modelling regional ground water flow. Consequently the ground water component includes only one upper, surficial aquifer assuming that leakage to a deep aquifer system is negligible.

Very limited geological information is available from boreholes in the delta. Along the western perimeter some data exist but recent consistent data are only to be found in the area covered by the Maun Ground Water Development project /5/. The data indicate alluvial sediments of predominantly sand but with a number of embedded silt or clay lenses. The lower permeable lenses do not have a regional extent but reflect local sedimentation conditions of the past. It has not been feasible to build a continuous 3-D geological model of the delta. On the larger scale local semi-confining layers are assumed to be of lesser importance. A homogeneous aquifer of constant thickness (15m) has been specified with a hydraulic conductivity of 10^{-5} m/s and an unconfined storage coefficient of 0.3.

'No flow' boundary conditions are specified along the perimeter of the delta.

Results of the ground water component of the ODMP hydrologic model should first and foremost be interpreted in terms of storage changes rather than as a representation of local, actual groundwater tables. The lack of local geological detail implies that model results of the distal fan area are to be viewed primarily as mean ground water storage levels.

5.8 Evapotranspiration

Different methods exist for simulating evapotranspiration (ET) using MIKE SHE. The simpler methods available apply a fixed ratio, ie a fraction of rainfall is lost to ET. This method cannot reflect the shifts between dry soil and inundation and, since the major part of evapotranspiration losses occurs in wet areas, it is not applicable for the delta.

The Kristensen and Jensen method /12/ simulates the actual rate of ET as a fraction of the potential rate of ET specified as model input. The simulated rate takes into account the actual soil moisture content, density of vegetation and flooding

conditions. The method is capable of addressing dynamic drying and wetting in response to the flood wave. The drawback is, however, the requirement of specifying potential ET rates in the delta. Reference ET estimates based on Penman-Monteith or similar are difficult to transfer to the range of natural vegetation types found in the delta, and climate time series from inside the delta are not available. Consequently, the uncertainties in potential ET estimates point to the more elaborate ET method using a Surface-Vegetation-Atmosphere Transfer module (SVAT).

Surface-Vegetation-Atmosphere Transfer Module

The SVAT module simulates the heat and energy fluxes between the atmosphere, a vegetation (or canopy) layer and a soil layer. Solar radiation along with differences in humidity and temperature drives heat fluxes between the two layers. A network of resistances is introduced to control the actual rate of heat fluxes.

The SVAT concept is widely used for meteorological studies /4/ but in this context a coupling with the Integrated Hydrologic Model has been developed (MIKE SHE SVAT, Appendix 1). An important derivative of the SVAT module is energy losses by ET processes and thus actual rates of evapotranspiration. The total ET losses are estimated from three individual terms representing evaporation from free water surfaces (flooded areas in the MIKE SHE Overland component), soil evaporation (soil moisture content of the MIKE SHE unsaturated zone component) and transpiration by the vegetation (soil moisture content of the MIKE SHE unsaturated zone component depending on vertical root mass distribution).

The SVAT module requires relatively detailed vegetation and climate time series inputs (see Table 5.2 and Table 5.3).

Table 5.2 : Climate Inputs to MIKE SHE SVAT Module

Climate Input	Distributed	Time Varying	Source of Data
Rainfall	No	Yes (Daily)	Maun/Shakawe stations (Botswana meteorological services) – gap filled
Solar radiation	No	Yes (Hourly)	Calculated from recorded sunshine hours in Maun (DMS) and solar angle - corrected from HOORC Met Tower data
Air temperature	No	Yes (Daily)	Shakawe station (Botswana meteorological services) – gap filled
Relative humidity	No	Yes (Daily)	Maun/Shakawe stations (Botswana meteorological services) – gap filled
Wind speed	No	No	Mean value for Maun (HOORC Meteorological Tower)
Air pressure	No	No	Mean value for Maun (Botswana meteorological services)

Rainfall is scattered in the delta and initially fully distributed data sets based on remote sensing data (cold cloud technique) for the area were reviewed. Comparisons with recorded rainfall rates from meteorological stations showed significant differences. Although distributed rainfall is useful, the difference in absolute values suggested using the rainfall time series from on-ground measurements. Shakawe

and Maun stations cover the longest periods and have fewer gaps, and were consequently used.

Table 5.3: Vegetation and Surface Inputs to MIKE SHE SVAT

Vegetation and Surface Input	Distributed	Time Varying	Source of Data
Leaf area index	Yes	Yes (8 days)	Estimated from MODIS satellite imagery (Appendix 3)
Albedo	Yes	Yes (8 days)	Estimated from MODIS satellite imagery (Appendix 3)
Root depth	Yes	No	Distributed from vegetation map /10/
Stomata Resistance	Yes	No	Distributed from vegetation map /10/
Vegetation height	Yes	No	Distributed from vegetation map /10/
Leaf width	Yes	No	Distributed from vegetation map /10/
Extinction coefficient	Yes	No	Distributed from vegetation map /10/
Subsurface roughness coefficient	Yes	No	Distributed from vegetation map /10/

Solar radiation has been calculated from time series of sunshine hours from Maun (Appendix 2). Comparison with solar radiation data from the HOORC meteorological tower indicated too high fluxes. Estimated values of 1,400W/m^2 at noon in December were scaled to comply with the measured range (up to approximately 1,200W/m^2).

Wind speed and air pressure are described by long term mean values based on meteorological data from Maun.

Leaf area index (LAI) describes the density of vegetation and is used in estimating transpiration losses from the surface of the vegetation (Figure 5.7). LAI is a key parameter in relation to ET losses. Time varying and distributed LAI values (8 day composites in 1km^2 grids) have been produced for the period 2000-2003 (Figure 5.8) /15/. Missing values due to for example cloud cover have been replaced by interpolation among neighbouring values. The LAI values are highly variable and mean values range from 0.5 to 5.5 for the period. Albedo describes the surface reflection of radiation to the atmosphere. Data sets were produced by means of MODIS satellite images for the same period as LAI data /15/.

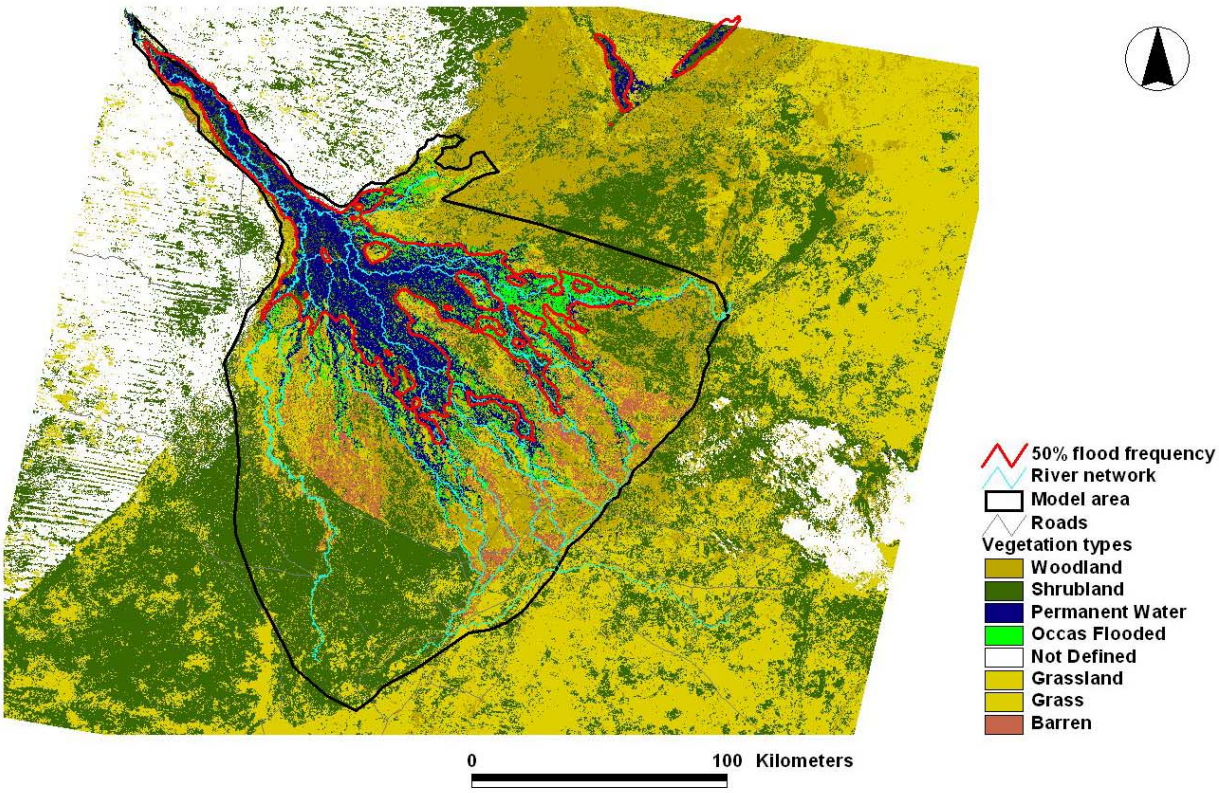

Figure 5.7: Vegetation Types

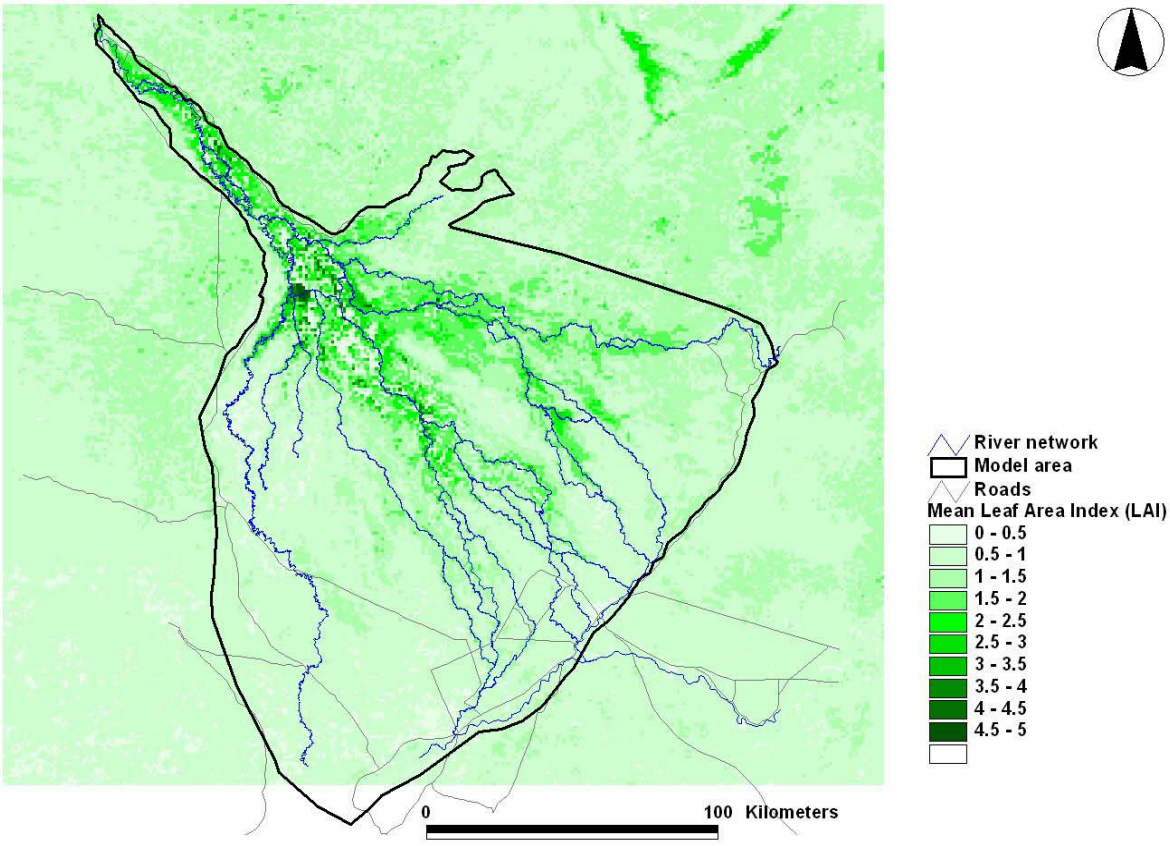

Figure 5.8: Mean LAI Values 2000-2003 According to Satellite Images

The SVAT module distinguishes evaporation from soil and ponded water on the surface as well as transpiration by vegetation. Evaporation from the vegetation is a function of state variables simulated by the model, eg soil water content and a number of vegetation specific parameters including root depth, stomata resistance, vegetation height, leaf width and extinction coefficient. The parameters have been distributed according to the vegetation classes, applying the following ranges:

- Root depth, 0.5–3.0m, where the lowest values are assigned to wetland areas and the highest values are applied in woodland
- Stomata resistance, 200–400, with higher resistance to evaporation in dry land vegetation species
- Vegetation height, 0.05–1.0m, minimum mean vegetation heights assigned to permanently flooded areas and maximum values for woodland.
- Leaf width, 0.02–0.05m
- Extinction coefficient, 0.5, global value

Application of the SVAT ET method proved useful in initial model runs but, due to the system of equations solved within the SVAT and the time steps applied to include diurnal variations, run times became excessive. As the model eventually will serve as a management tool to analyse different scenarios, it was decided to reduce run times by using a combination of the Kristensen and Jensen method and the SVAT module. The SVAT module is used to simulate the potential rates of evapotranspiration for the Delta prior to running the integrated hydrologic model for the Delta. Time series of potential evapotranspiration derived from the SVAT module run are specified as input for the hydrologic model and the Kristensen and Jensen method simulates the spatial and temporal variation in actual evapotranspiration rates. Actual rates of ET simulated by the Kristensen and Jensen method are always less than or equal to potential ET rates depending on the actual soil moisture conditions, flooding, vegetation and soils.

6. MODEL CALIBRATION

6.1 Introduction

The purpose of model calibration is to select and adjust model parameters to obtain a satisfactory agreement between model simulation results and observed field data. The level of calibration expresses the ability of the model to simulate key processes in the Delta, and if the conceptual model is appropriate with respect to describing the Delta hydrology.

The ODMP hydrologic model includes a large number of parameters describing hydrologic characteristics distributed across the delta. In order to obtain model results that reflect actual field observations, the model parameters are subject to adjustments as part of the calibration process. The parameter ranges in the calibrated model must, however, be physically reasonable, ie within pre-specified ranges, to support the further use of the model for impact assessment.

The complexity of the delta compared to the limited available field data for calibration makes accurate calibration of individual areas or river sub-systems difficult. There are limited bases for assigning local parameter values and no observation data to verify the model performance. Consequently, the model performance is evaluated partially by quantitative and partially by qualitative assessments, looking at the larger scale model outputs.

Calibration of the Okavango Delta hydrologic model has been targeted towards specific outputs of relevance to the subsequent model applications (Table 6.1).

Table 6.1: Model Outputs, Performance Requirements, Calibration References and Priorities

Model Result	Requirement	Calibration Reference	Priority
Flood extent	Simulate extent of permanently and temporarily flooded areas in the delta	Comparison with flood extent derived from satellite images	1
Water balance	Simulate total water balance including distributed time-varying ET rates , losses to the subsurface, storage changes and discharges	Gauged continuous discharges downstream the delta.	2
Water levels	Simulate mean water levels and water level changes	Gauged datum referenced water levels	3

Parameter estimation (automatic calibration) describes the process of deriving optimal calibration parameter sets by pre-defined calibration targets, parameter intervals and statistical performance criteria. Parameter estimation does not include any physical reasoning by the modeller in the process and requires a large number of calibration model runs. Parameter estimation tools are available with the MIKE SHE–MIKE 11 modelling system (eg PEST or Shuffled Complex Algorithm), but the run times (approximately 4 hours to run one year on a standard PC) do limit automated parameter estimation with respect to the ODMP hydrologic model. The manual calibration process is in principle not different from parameter estimation but involves

subjective evaluation and guidance of the calibration process based on modeller experience and physical understanding. A manual calibration approach has been adopted.

6.2 Data Used in Calibration

Flood extents derived from NOAA AVHRR satellite imagery have been applied in the calibration process /6/. A large number of flood maps covering the entire delta has been generated for every tenth day for the period 1985-2000.

The flood maps have been produced at a 1km^2 resolution. Due to cloud cover and potentially mismatching single grid cell values, manual corrections were made. Where flooding only partially covers grid cells the grid has been assumed flooded if more than 25% of the grid cell area is inundated according to the images.

Flood maps covering mainly the flood season were later on provided by HOORC. The period for which satellite images are available has been extended to March 2005. The new images have not been corrected for cloud cover.

The satellite images have been processed to produce flood frequency maps. Permanently flooded areas, frequently flooded areas, occasionally flooded areas and dry land areas are delineated to guide the calibration process. Since flood extent and spatial flooding patterns vary by year and by season, flood frequency maps have been used to calibrate permanently dry, permanently flooded and seasonally flooded areas. In addition, flood extents at particular dates may be compared. In the comparison it is, however, important to stress that the processing of pixels, assumptions on when to assign flooding to a partially flooded area and cloud cover introduce uncertainty in the observation data set. In the model results flood water levels are computed as a spatial mean for 1km by 1km grid cells disregarding sub-scale variability in the topography, and a grid cell is assumed flooded when the water level exceeds 0.01m. Consequently the comparison between simulated and observed flooding is only approximate.

6.3 Model Parameters

The Integrated Hydrologic Model comprises a long list of parameters, which at varying degrees are distributed across the model area. Consequently the potential number of parameters and parameter combinations is high. It is, however, only feasible to consider certain of the potential parameter sets in calibration. The effect of various parameters on model results is highly variable, which is used to single out the parameters of paramount influence. Sensitivity runs may serve to determine the response of specific model outputs to changes in model parameters. Although no systematic (and time consuming) sensitivity analysis was carried out, initial model runs served to verify that parameters singled out for calibration were in fact the dominant parameters with respect to model sensitivity (Table 6.2).

Calibration aims at adjusting model parameters until a satisfactory match with calibration references is obtained. The model input, for example climate time series, and model structure, ie model geometry in terms of surface topography and river cross section, is fixed, which implies that any inconsistencies may be compensated by the choice of parameters.

Selection of the calibration period is restricted by two remote sensing data sets. The LAI data based on MODIS data are only available from for 2000-2004. The flood extents derived from satellite imagery cover the period 1985-2004. Consequently model calibration using actual LAI values and comparing against actual flood extents is only possible for 2000-2004. The period 1.1.2000 – 1.3.2004 has been selected.

Table 6.2: Calibration Parameters

Model Result	Processes	Key Parameters And Ranges
Flood extent	River/channel flow Overland flow River-flood plain spills	Channel Manning number, 5-30 $m^{1/3}/s$ Overland Manning number, 1-5 $m^{1/3}/s$ (Topography and river geometry crucial)
Water balance	ET losses Subsurface storage	Vegetation height (wet land ET), 0.05-1.0m Stomata Resistance (dry land ET), 200-400 Extinction coefficient (general ET), 0.4-0.7 (Climate input time series crucial)
Water levels	River/channel flow	(Datums of cross sections crucial)

The period covers four full hydrologic years including annual variations in climate and inflow to the Delta. Within this period it is possible to test the model performance in terms of dynamic flood extent and water balance, which are the main objectives. Given the climatic cycles and available inflow time series a longer calibration period would be preferable to support statistical analysis of model output time series and test the ability of the model to represent longer dry or wet periods covering several years. The selected period is, however, considered sufficiently long for calibration purposes.

6.4 Calibration against Flood Extents

Calibration against flood extents includes :

- Comparison of time series of total flood extent across the Delta from model results and interpreted satellite data, respectively
- Comparison of simulated flood extents against flood frequency maps; model performance evaluated by ability to represent permanently flooded, occasional flooded and non-flooded areas
- Comparison of flood extents at a particular point in time

Figure 6.1 shows the simulated and observed total flood extents in the Okavango Delta and the upstream discharge at Mukwe, which is the inflow boundary condition in the river flow model. The satellite images show flooding in the range of 5,000-10,000km^2, while the model simulates flooded area with 4,000-11,000km^2. The model simulated the general trend in total flooding found from satellite images (RMS equal to 306km^2). No systematic bias in the simulated flood extent in terms of temporal trends is observed, ie increasing or decreasing deviations through the simulation period.

According to Figure 6.2 the model performs well for both low and high flood ranges in the calibration period, without systematic underestimation or overestimation of flood extents. Apparently the model represents the low flood range slightly better than the high flood range for the period considered, but there is no systematic bias for any of the ranges. A correlation coefficient of 0.9 is indicative of a satisfactory agreement between simulation and observation data.

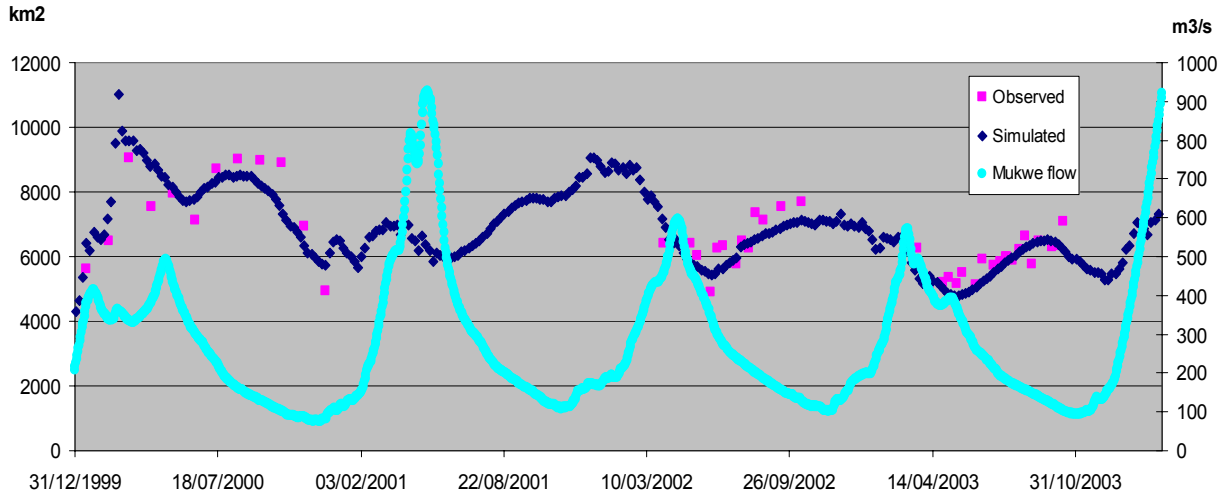

Figure 6.1: Simulated and Observed Total Flood Extents

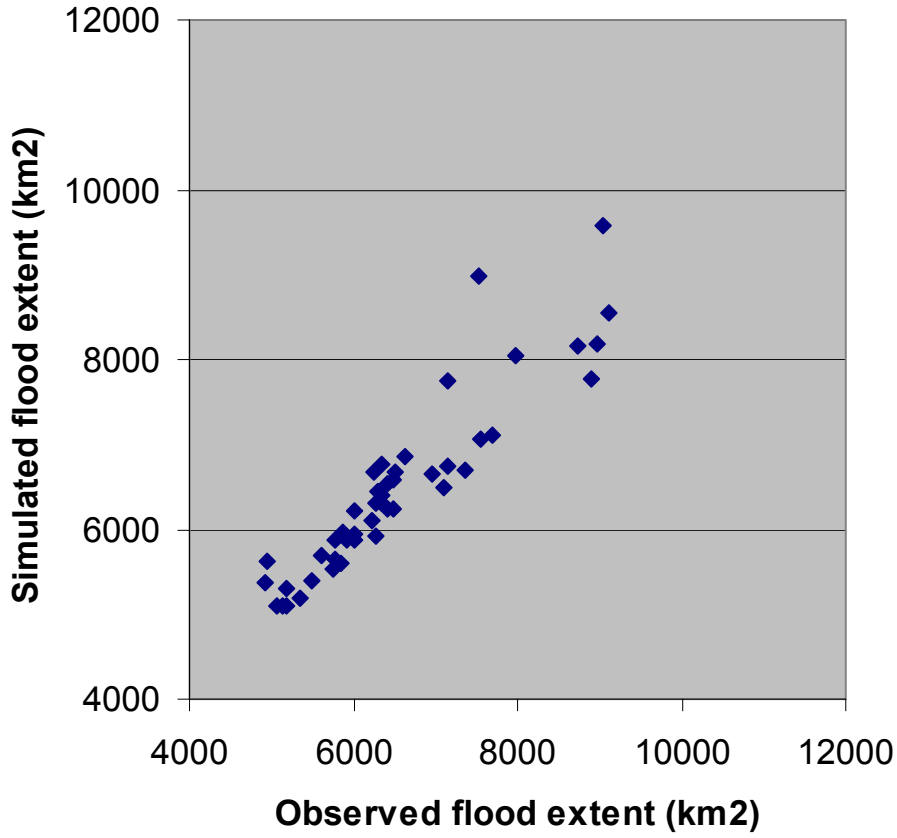

Figure 6.2: Simulated versus Observed Flood Extents

Figure 6.3 shows simulated flood frequencies for the calibration period (2000-2004) and Figure 6.4 shows flood frequencies based on interpretation of satellite data for the period 1985-2000. It is not possible to produce directly comparable flood frequency maps for the calibration period, since only restricted periods are covered by the observation data. This implies that the figures can serve only roughly to compare flood patterns under the assumption that annual flood events have not been fundamentally different for the two periods despite differences in climate and inflows.

Flooding in the Panhandle is similar, which is not surprising given the fault lines effectively constraining the flood extents. Along the Ngoqa-Khwai branch the model simulated flooding extends further north, which is likely attributed to the location of blockages and spills, and the accuracy of the topographic model. The model simulated flooding also extends further downstream on the Khwai where observed data suggest that more water is spilled further upstream. On the Jao-Boro flooding patterns are similar with some differences along the downstream Boro. The flood plain extends further downstream according to satellite data whereas the model produces small, scattered areas of flooding which do not appear in the satellite data. On the Crescent-Thaoge approximately the same areas are flooded with the exception that the simulated flooded area extends further downstream on the Matsebe. Such differences are, however, not conclusive as flood frequencies vary depending on the period considered.

Figure 6.5 and Figure 6.6 show the actual flooding simulated by the model at particular selected dates. The dates are chosen to represent 'high flood level' (March 2000) and 'low flood level' (May 2003) from the calibration period. The figures show flooding depth in the range from 0.4m, which reflects the propagation of the flood wave, the actual distribution of flood water volumes and the underlying surface elevation represented by the topographical model. The deep inundation is generally restricted to the Panhandle and proximal fan. As the model results represent average flooding in 1km by 1km squares, locally depressed areas may not appear explicitly from the figures.

Table 6.3and Table 6.4 compare simulated and observed flood extents in the main sub-basins of the Delta. A 'high flood level' situation and a 'low flood level' situation have been selected. The total flooded area simulated by the model is approximately 4% higher in the 'high flood level' situation than observations, and 7% lower in the 'low flood level' situation. Under 'high flood level' conditions the largest deviation between simulated and observed flood areas is found in the Crescent-Thaoge subsystem (18%), whereas the largest deviation is found in the Panhandle during the 'low flood level' situation (10%). The model appears to overestimate flooding along Crescent-Thaoge. For the remaining subsystems no systematic trend towards underestimation or overestimation was found.

Table 6.3: Total Flooded Areas from Model Results and Satellite Image ('high flood level', March 2000)

Zone	Simulated Flooded Area (km2)	Observed Flooded Area (km2)	Deviation (%)
Panhandle	832	861	3.4
Nqoga-Maunachira-Khwai	3,892	3,867	0.6
Jao-Boro	3,807	3,612	5.4
Crescent-Thaoge	850	722	17.7
Total	**9,381**	**9,062**	**3.5**

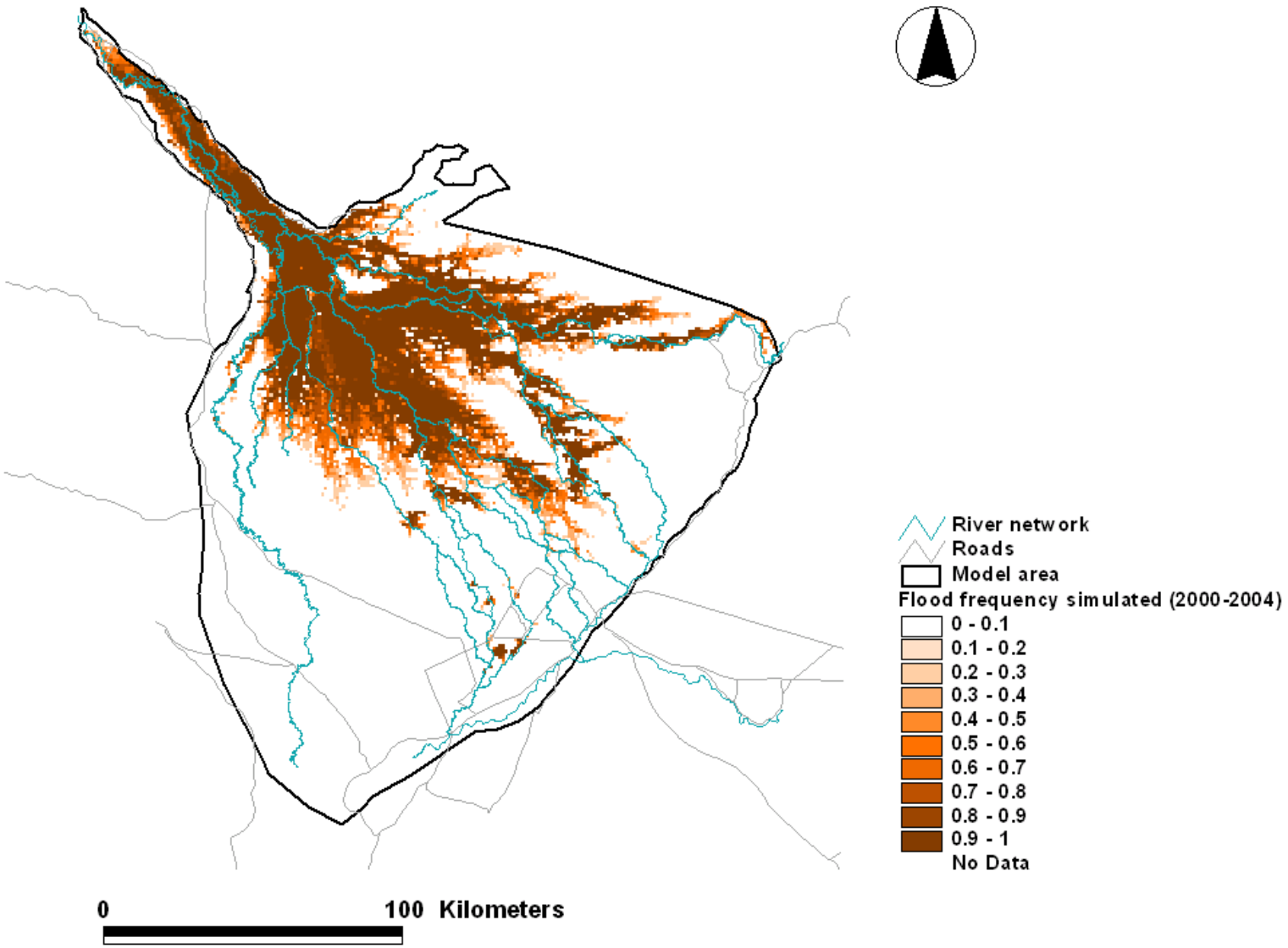

Figure 6.3: Simulated Flood Frequency for Calibration Period (2000-2004)

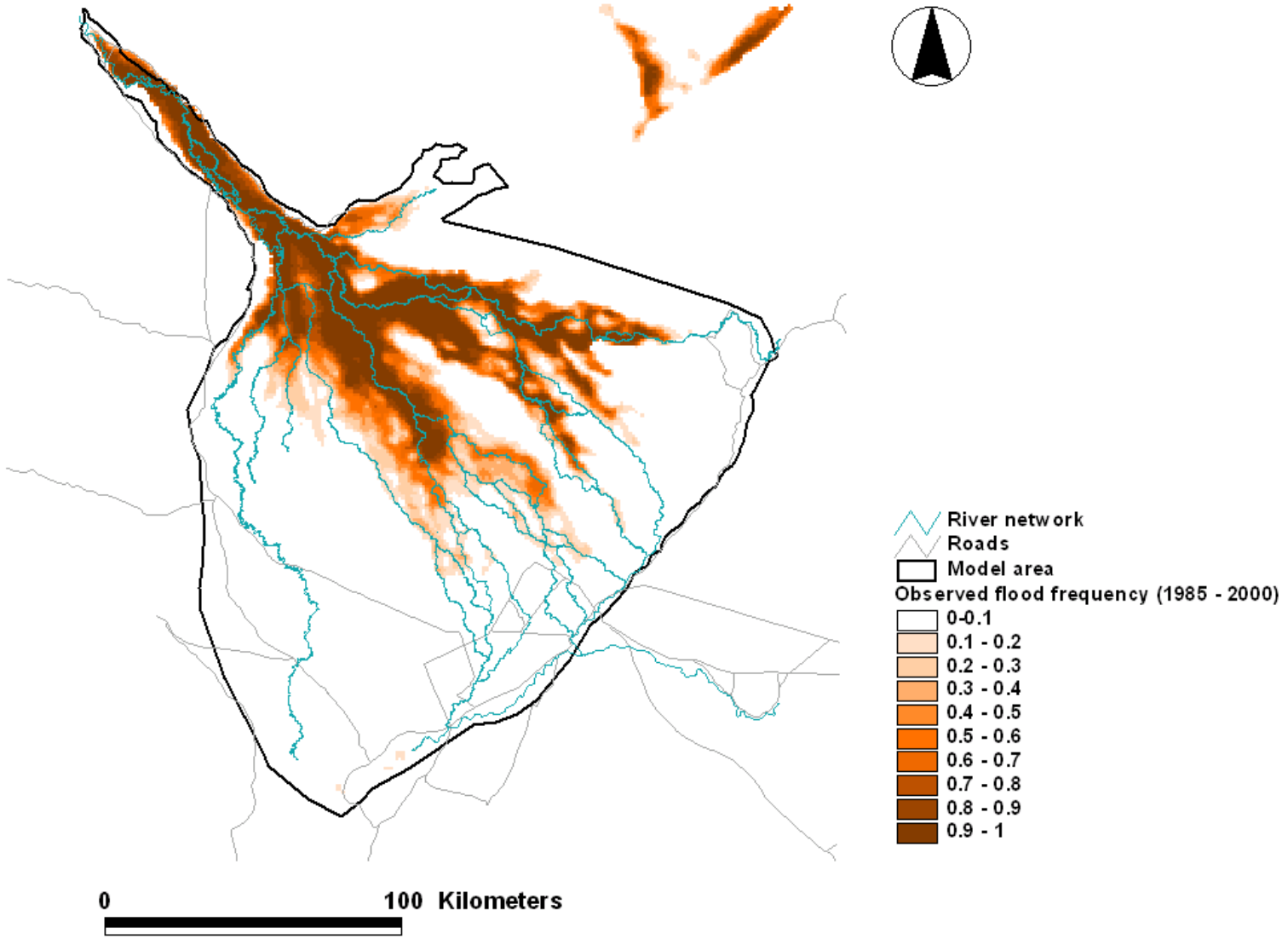

Figure 6.4: Flood frequency Derived from Satellite Images (1985-2000)

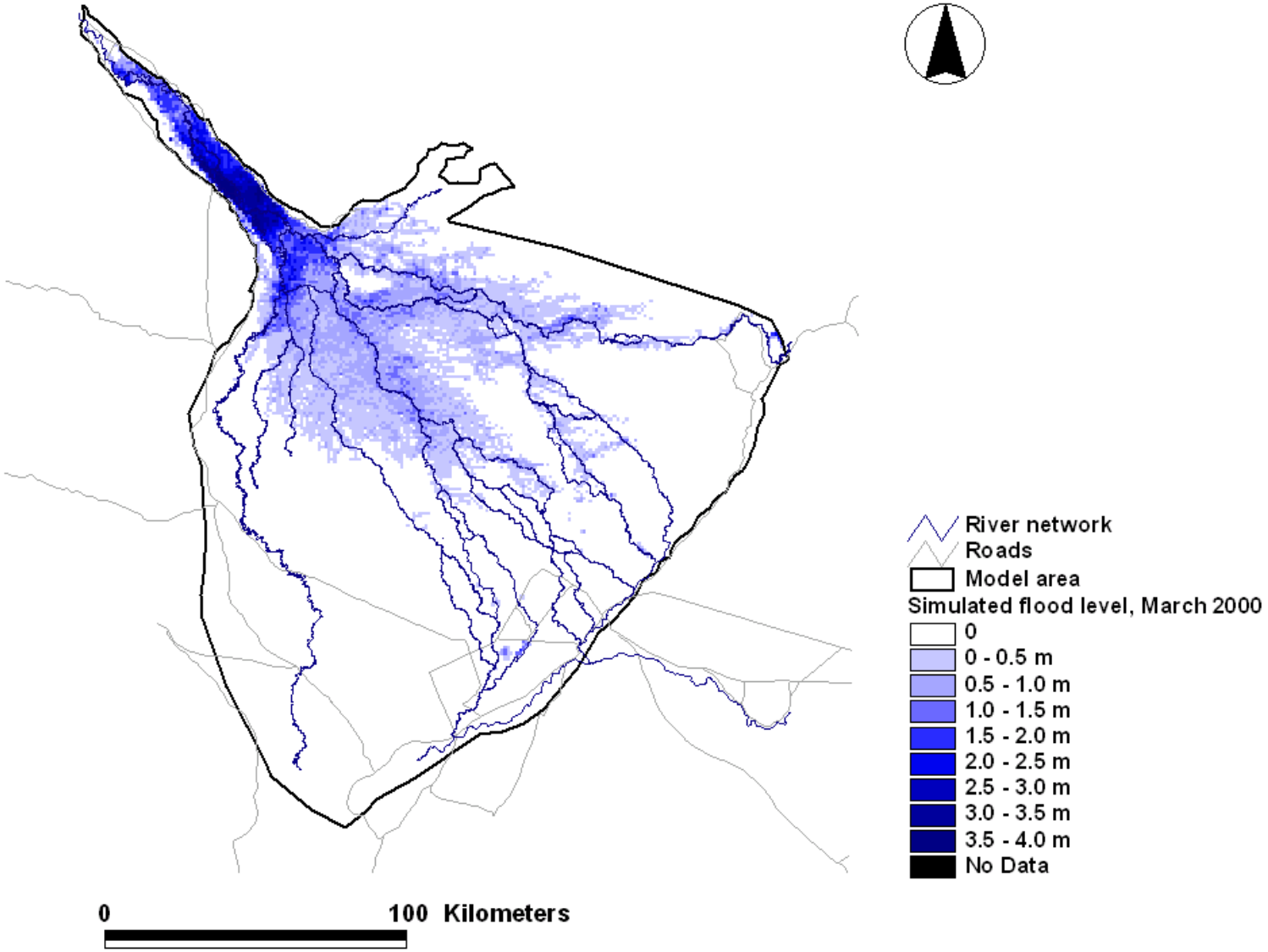

Figure 6.5: Simulated Flood Extents during 'High Flood Levels' (March 2000)

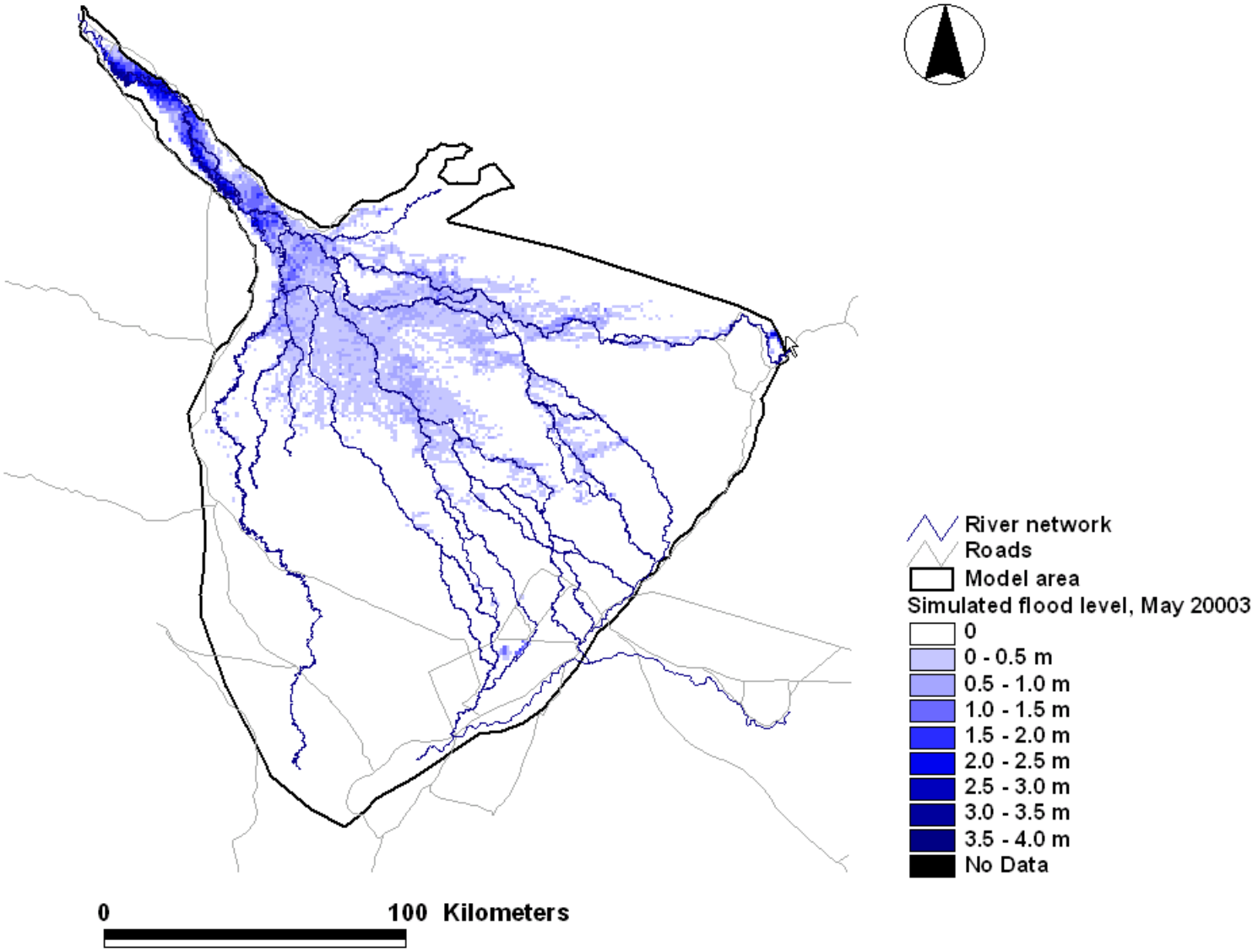

Figure 6.6: Simulated Flood Extents during 'Low Flood Levels' (May 2003)

Table 6.4: Total Flooded Areas from Model Results and Satellite Image ('low flood level', May 2003)

Zone	Simulated Flooded Area (km2)	Observed Flooded Area (km2)	Deviation (%)
Panhandle	897	998	10.1
Nqoga-Maunachira-Khwai	1,938	2,101	7.8
Jao-Boro	1,577	1,695	7.0
Crescent-Thaoge	439	434	1.2
Total	**4,851**	**5,228**	**7.2**

6.5 Calibration against Discharges (Water Balance)

Calibration against discharges addresses downstream river discharge in a water balance perspective. Surface water may discharge across delta boundaries in the Khwai, Thaoge and Boteti rivers. The Khwai River has not been known to flow beyond the delta boundary as a topographic threshold limits flow under present climatic conditions, though flow to the Mababe Depression is a possibility.

The Thaoge has carried significant water up till less than 100 years ago. Due to major shifts in the flow distribution at upstream channel splits and severe vegetation blockages, water entering the Thaoge spills along the upstream reaches. The downstream reaches remain dried out and no flow leaves the delta through the Thaoge.

The Thamalakane River collects flow from several distributaries in the far downstream delta. The river runs along the Thamalakane fault, and in high flood years discharges through a break in the fault to the Boteti River.

The annual flood wave propagates slowly through the delta. Gauged water levels suggest travel times in the order of one month from Mohembo to the downstream Panhandle, and an additional 2 months to the downstream delta around Maun.

Figure 6.7 and Figure 6.8 show an example of the simulated discharges and time lag of an annual flood wave propagating through the Okavango Panhandle, and through the Jao-Boro channel respectively. The rising leg of the hydrograph at Mohembo and downstream of the Panhandle shows a delay of approximately 6 weeks, with a further 8 weeks through the Jao-Boro. The simulated flow includes flow in the main channel and a 1km section of the adjacent flood plain. In the Boro downstream, the flood wave appears totally attenuated when plotted with the upstream discharge.

The simulated discharges compared with gauged flow data from a number of locations show, in most cases, agreement in terms of long term accumulated flow, which is important with respect to the water balance (Figure 6.9, Figure 6.10 and Figure 6.11). The variation in time of discharge is generally not captured by the model in detail and in some cases with considerable time lag. The comparison with flows in the simulation model covering the channel, and partially the flood plain with gauged data in stations only covering the main channel section, make it difficult to

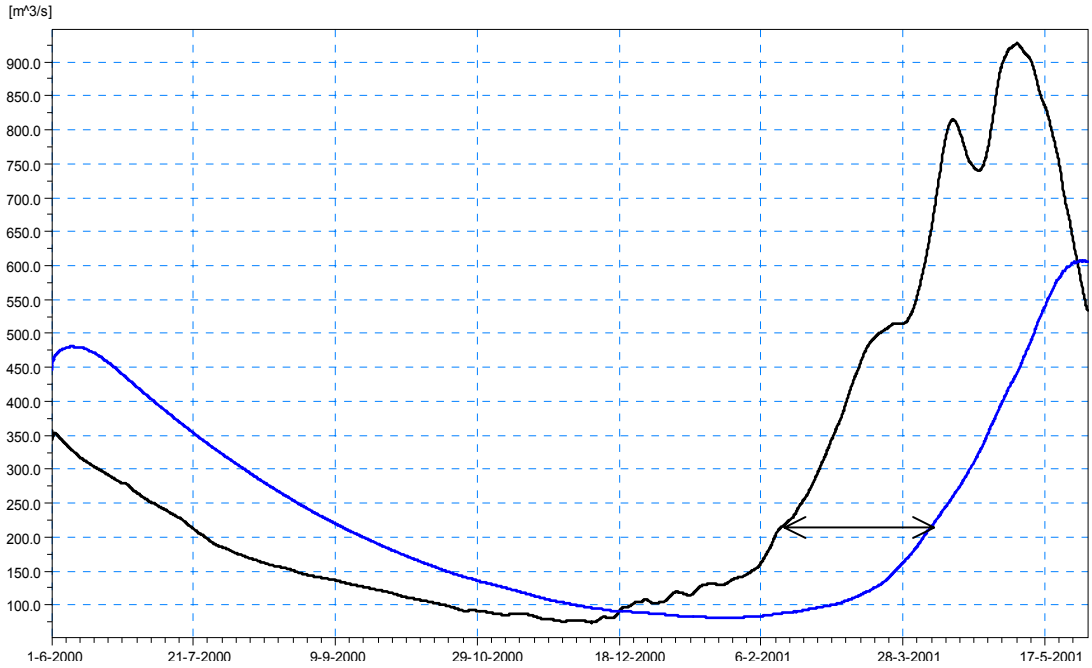

Figure 6.7: Example of Simulated Discharges in Okavango River from Upstream to Downstream in Okavango Panhandle

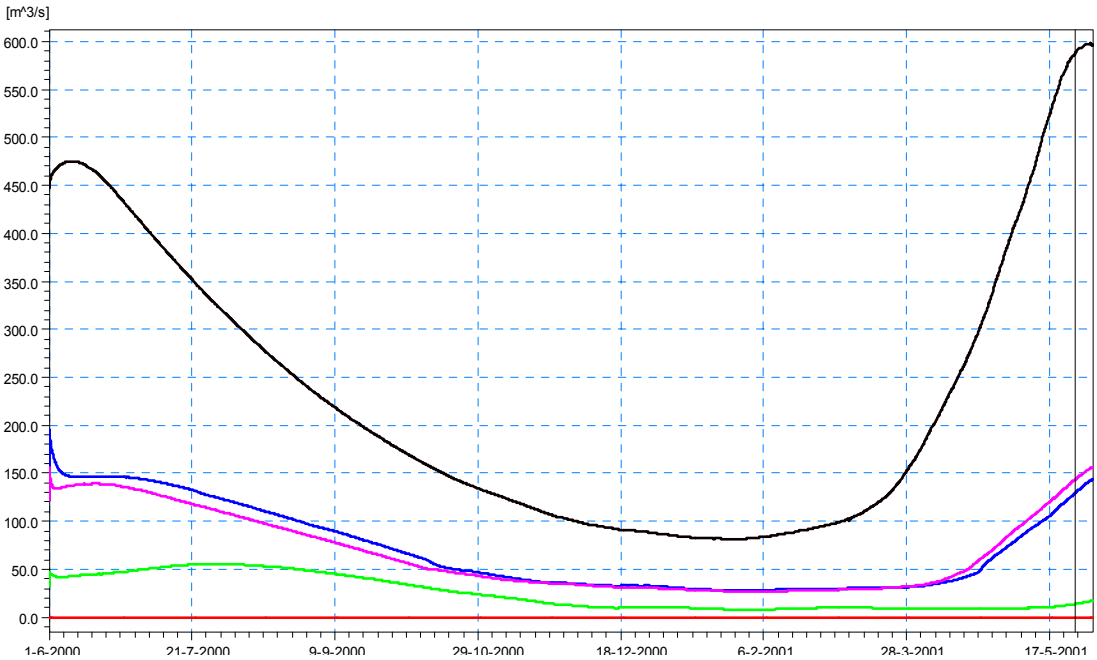

Figure 6.8: Simulated Discharges in Okavango River (downstream of Okavango Panhandle) and along Jao and Upstream/ Downstream Boro River.

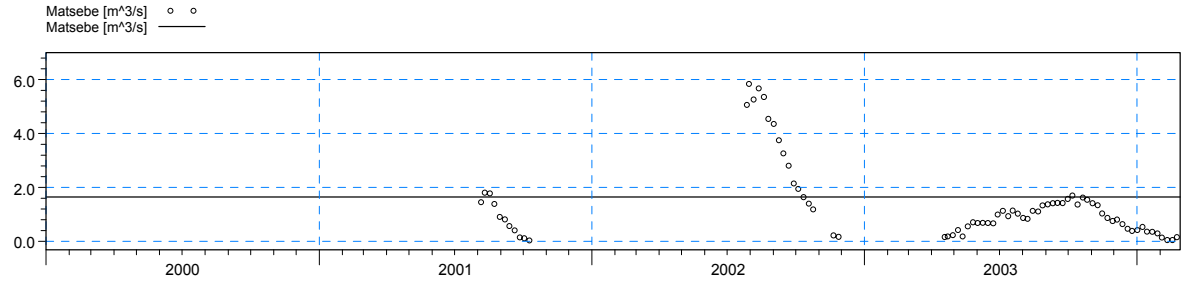

ME=-0.319718
MAE=1.06854
RMSE=1.4095
STDres=1.37276
R(Correlation)=-0.16049
R2(Nash_Sutcliffe)=-0.0543495

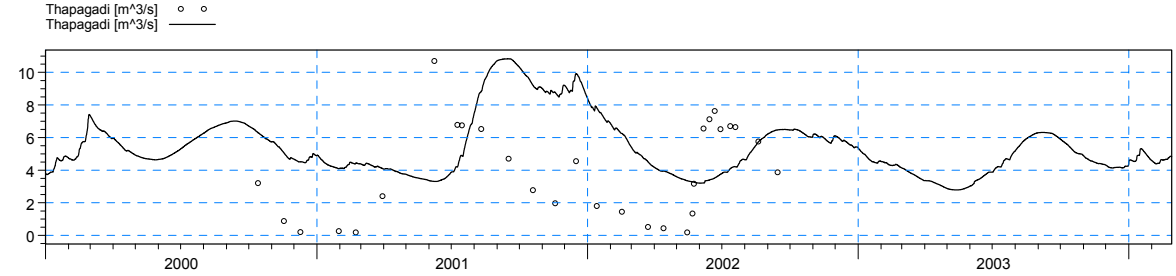

ME=-0.68665
MAE=3.3113
RMSE=3.70621
STDres=3.64205
R(Correlation)=-0.137597
R2(Nash_Sutcliffe)=-0.911066

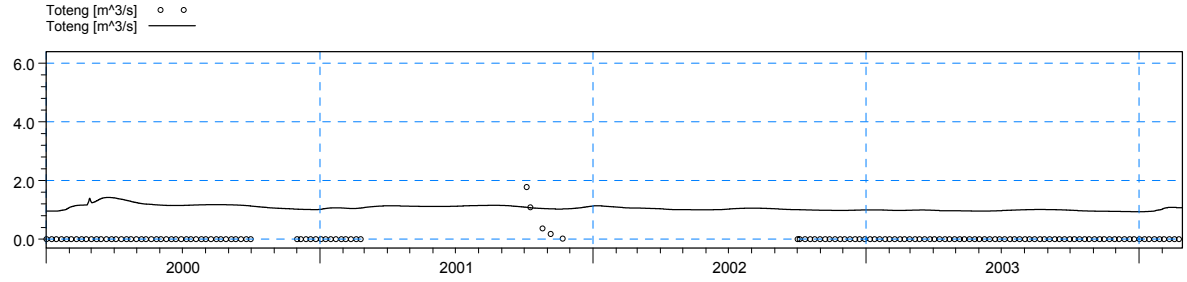

ME=-1.04143
MAE=1.044
RMSE=1.05297
STDres=0.155405
R(Correlation)=0.0123358
R2(Nash_Sutcliffe)=-93.7241

Figure 6.9: Simulated versus Observed River Flows (Matsebe, Thapagadi, Toteng)

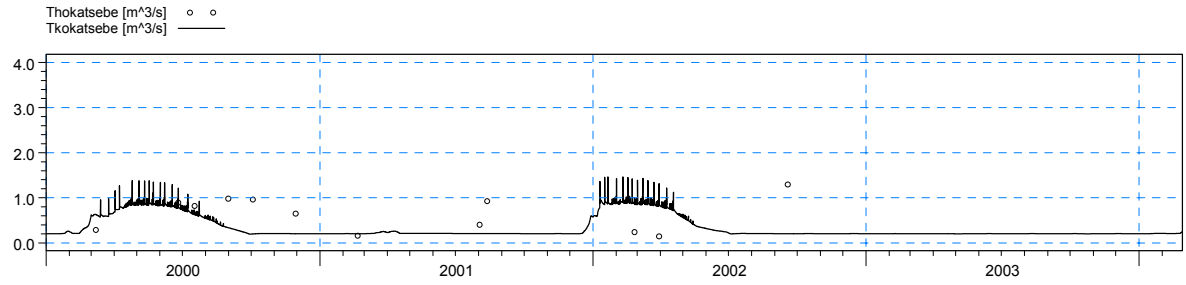

ME=0.176049
MAE=0.497194
RMSE=0.588984
STDres=0.562057
R(Correlation)=-0.3533
R2(Nash_Sutcliffe)=-1.53999

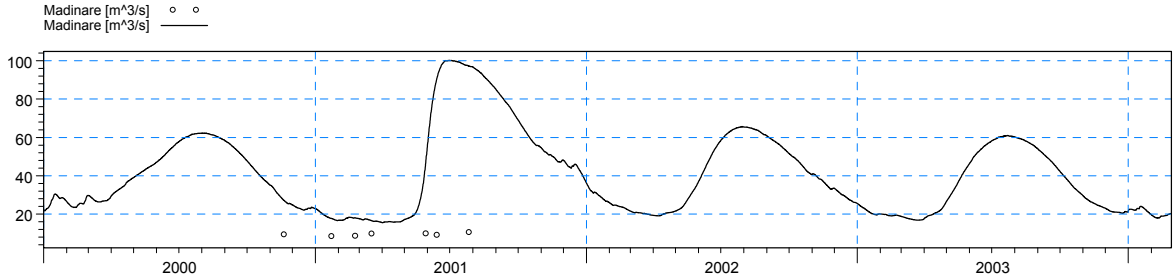

ME=-35.3993
MAE=35.3993
RMSE=47.8523
STDres=32.1983
R(Correlation)=0.545648
R2(Nash_Sutcliffe)=-5432.6

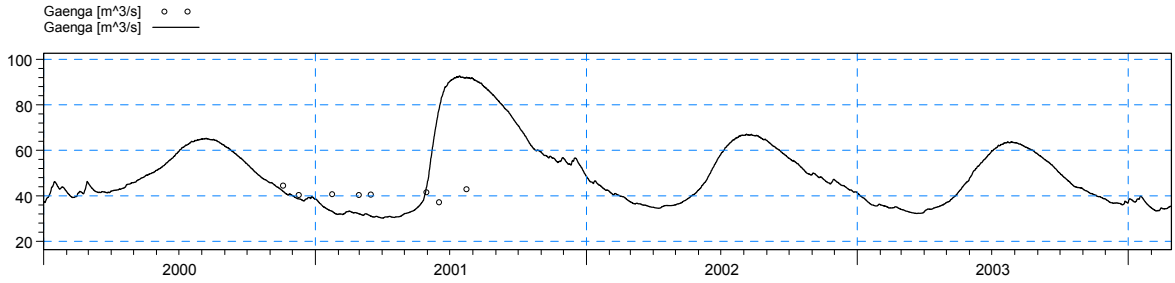

ME=-7.83794
MAE=15.1947
RMSE=23.241
STDres=21.8795
R(Correlation)=-0.0807375
R2(Nash_Sutcliffe)=-134.397

Figure 6.10: Simulated versus Observed River Flows (Thokatsebe, Madinare, Gaenga)

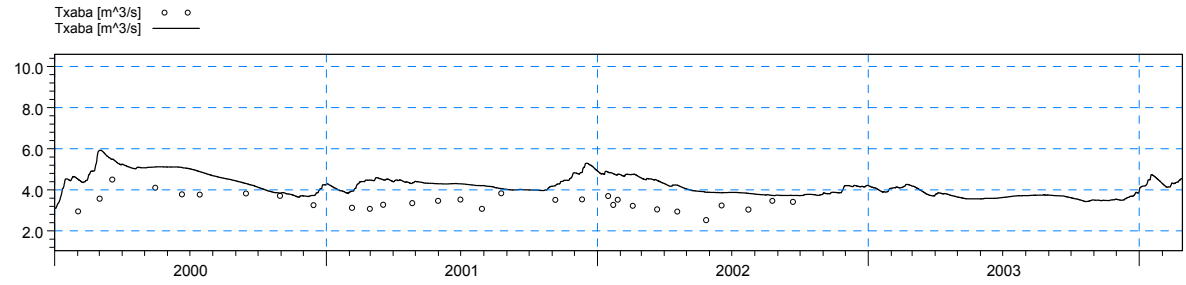

ME=-1.03881
MAE=1.03881
RMSE=1.15222
STDres=0.498485
R(Correlation)=0.4505
R2(Nash_Sutcliffe)=-8.04456

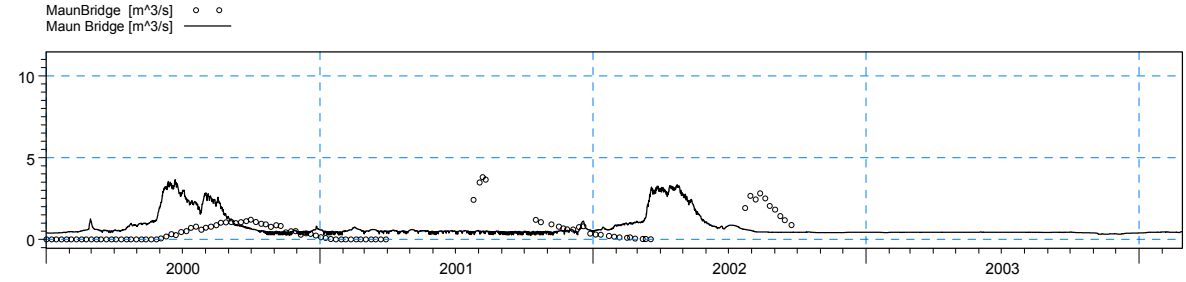

ME=-0.369396
MAE=0.873409
RMSE=1.16045
STDres=1.10008
R(Correlation)=-0.0507526
R2(Nash_Sutcliffe)=-1.50267

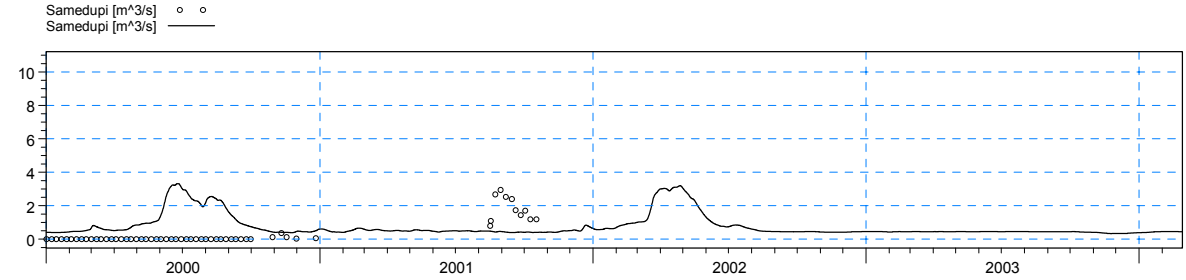

ME=-0.884438
MAE=1.31777
RMSE=1.59569
STDres=1.32816
R(Correlation)=-0.308142
R2(Nash_Sutcliffe)=-3.67455

Figure 6.11: Simulated versus Observed River Flows (Txaba, Maun Bridge, Samedupi)

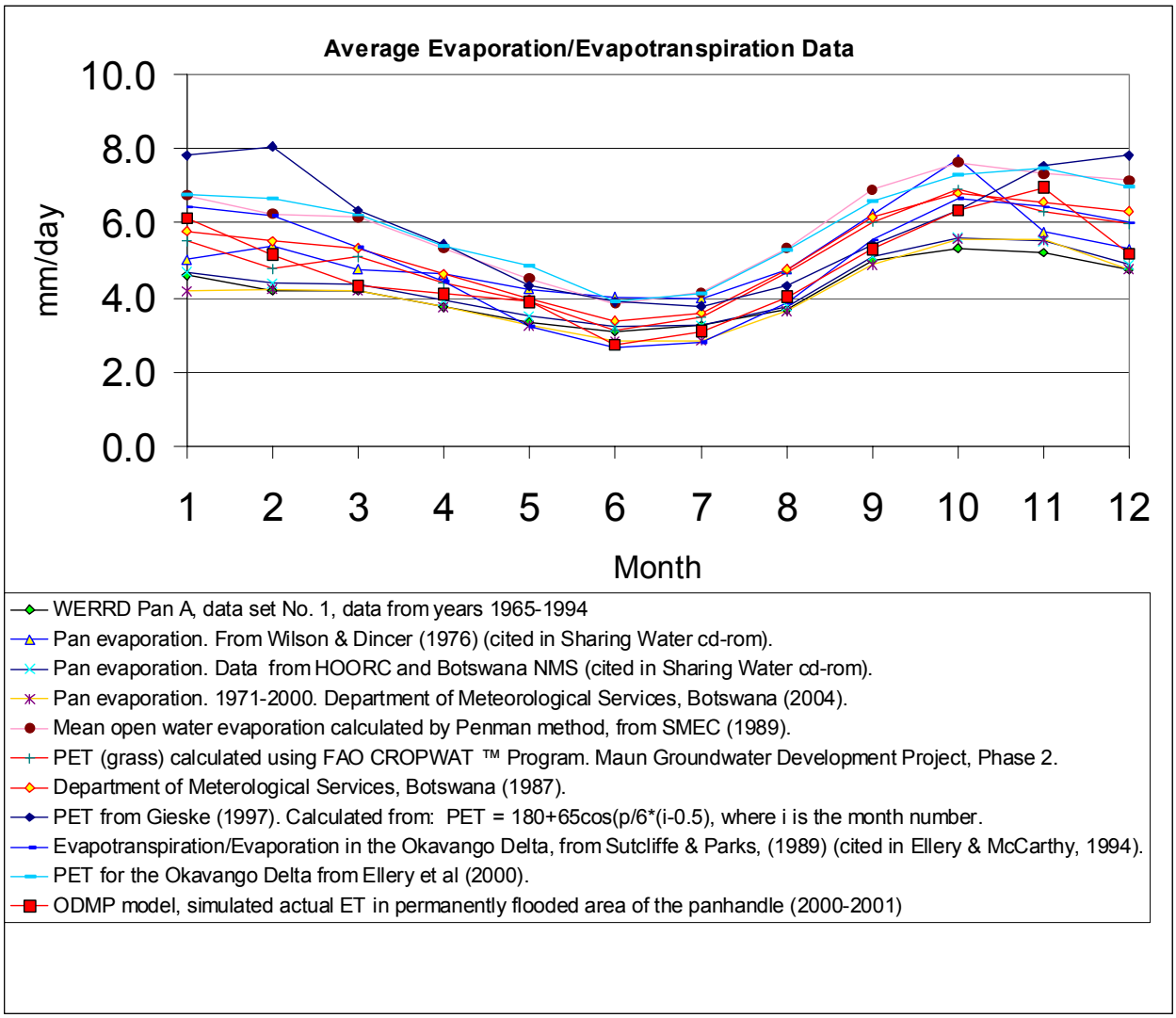

Figure 6.12: Annual Fluctuation in Simulated Actual Rates of ET in a Permanently Flooded Area compared to Pan Evaporation Data

assess the degree of accuracy. The comparison between the gauged and simulated delta outflows at Maun Bridge on the Thamalakane and Samedupi on the Boteti (Figure 6.11) shows a large temporal shift. Examination of the simulated discharges in the lower Boro shows the upstream flood wave is amplified and transformed by the local rainfall-runoff in the following rainy season. On this basis it is uncertain the extent to which the model results are applicable in evaluating local temporal flow fluctuations.

Although being the most important factor in the water balance, evapotranspiration cannot be directly calibrated. The performance of the ODMP hydrologic model ET component can be assessed by looking at field measurements, the total water balance of the delta and individual time series of simulated ET losses. Figure 6.12 compares a wide collection of evaporation and evapotranspiration data with evapotranspiration rates simulated by the Okavango Delta Integrated Hydrological Model. The simulated seasonal variation of ET is in agreement with the average annual fluctuation found in field data and estimated ET rates. The simulated rates fall within the ranges of the different estimated ET rates. The range of 1-2mm/day illustrates the difficulties of deriving accurate and representative ET rates of the Delta in general, and the differences between corrected field data and empirical methods.

Direct comparison is difficult but the figure shows that simulated values are in general agreement with ET rates from other sources.

The simulated ET loss for varying wet and dry conditions is of particular interest as it demonstrates the ability of the model to simulate the seasonal dynamics across the Delta. Figure 6.13 shows simulated rates of ET in three locations in the Panhandle. The three locations are characterised by being permanently flooded, occasionally flooded and non-flooded. Depths of flooding are shown (dashed lines) and the response of the actual evapotranspiration to flooding is distinct.

The permanently flooded area (full black line) has high ET rates close to the potential ET rates with seasonal variation, which is mainly controlled by differences in solar radiation. The dry land location (full red line) has much lower ET losses approaching zero in September, when soil evaporation is the only non-zero ET term. The ET rates of the occasionally flooded area (full green line) are similar to those of the dry land as the soil water content is slightly higher allowing higher ET rates. When the area is flooded (March-May 2001) the ET rates increase significantly and the evaporation from overland water becomes the dominant ET loss term. The figure illustrates the basic behaviour of the ET simulation module as a function of varying hydrologic conditions.

Table 6.5 shows the total water balance in millimetres for the entire model area including dry land, occasionally flooded and permanently flooded areas. The total water balance for the delta during the calibration period shows an actual ET loss of 3,013mm, which is only 81mm less than the sum of rainfall and upstream river discharges (3,094mm). An increase in stored water of 74mm during the period including both subsurface and surface water leaves only 7mm for downstream

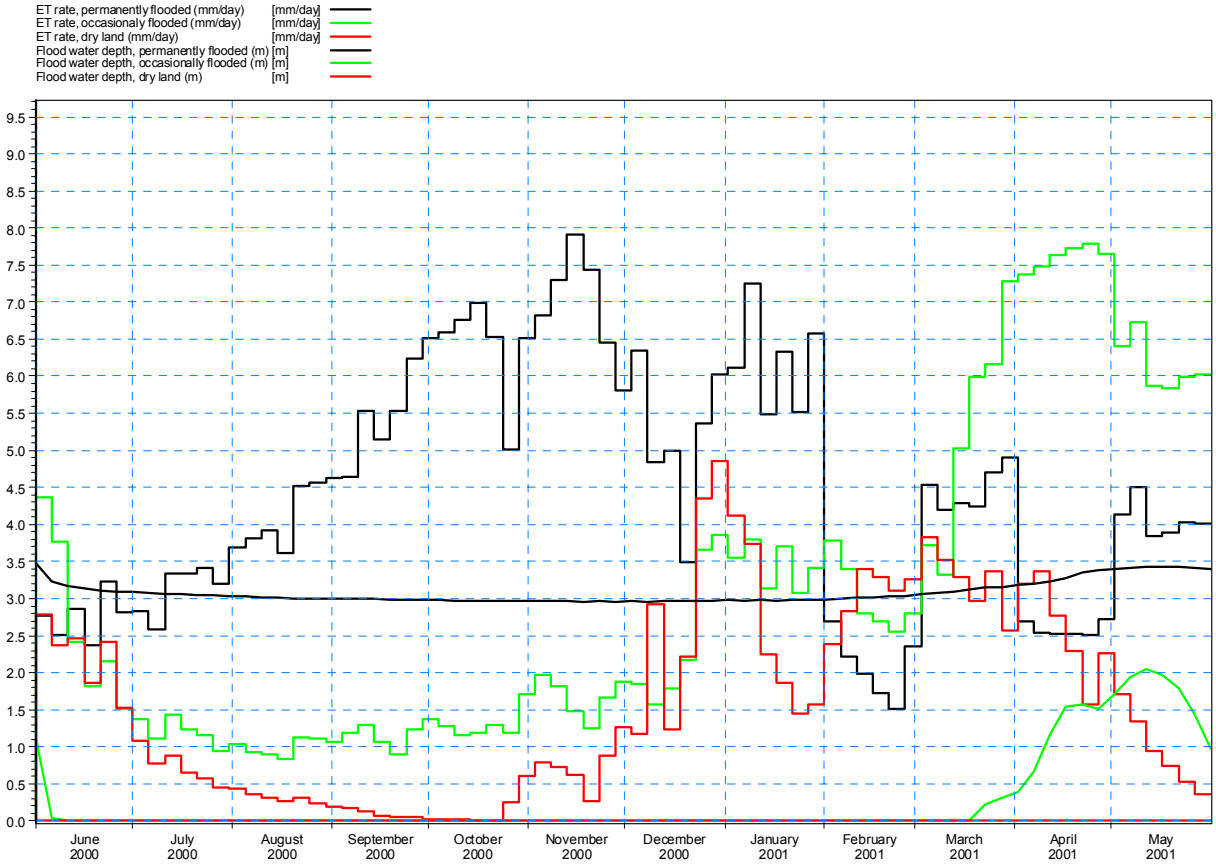

Figure 6.13: Simulated ET Dynamics in response to Wet and Dry Conditions (Okavango Panhandle)

discharge out of the Delta. A complete water balance for the Okavango Delta is produced by the integrated hydrologic model with the exception of a 1mm error. The results confirm the conceptual model where ET loss is the dominant water balance term controlling the total extent of flooding. Compared to the limited discharge through the Delta the storage capacity of the flooded areas is high, which implies that despite higher annual inflows to the Delta most of the additional volume is stored in the flooded areas and only a limited proportion adds to downstream discharges.

Table 6.5: Simulated Total Water Balance for Calibration Period (1.1.2000-1.3.2004)

Water Balance Component	Volume (Mm^3)
Inflow	1,301
Rainfall	1,794
Evapotranspiration	-3,013
Outflow	-7
Surface water storage change	-42
Subsurface storage changes	-32
Water balance error	1

.

7. CONCLUSIONS AND RECOMMENDATIONS

7.1 Development of ODMP Integrated Hydrologic Model

The ODMP Integrated Hydrologic Model based on the integrated modelling system MIKE SHE–MIKE 11 represents the most comprehensive simulation model of the Okavango Delta. Addressing all major hydrologic processes related to subsurface flow, the surface water flow and the evapotranspiration losses to the atmosphere provides a unique hydrologic modelling tool capable of addressing the multiple interrelated hydrologic processes of the area.

The conceptual model, forming the basis for the numerical model, depends to a large degree on the extensive scientific work carried out in the delta in the past. The findings of a number of research projects during the last three decades have provided the conceptual basis for the ODMP hydrological model. The major processes and physical mechanisms controlling the delta hydrology are represented in the Integrated Hydrologic Model.

The conceptual model has been implemented in a MIKE SHE-MIKE 11 numerical model with a physically based representation of major flow and exchange processes.

7.2 Model Calibration

The approach to model calibration has been determined from the pre-defined calibration targets. Following acquisition of additional satellite images to determine dynamic flood extents, the calibration period was extended to cover the period 1.1.2000-1.3.2004.

The model results are, in order of priority, evaluated against observed total flood extents and downstream river discharges from a water balance perspective.

Flood frequency maps based on satellite images are used to separate permanently flooded, occasionally flooded and dry land areas of the delta. Simulated flood extents during expansion and retreat of the flooded areas generally fall within the three land categories. The general flood pattern is thus in agreement with observations. A more direct comparison between simulated and observed flood frequencies is not possible due to restrictions on model input and long model simulation run times.

Comparison of the observed and simulated flood extent at a particular time (September 2000) shows that the total flood area in the delta is overestimated by approximately 4% for the entire model area. The results indicate total simulated flooded areas to be moderately overestimated in the Nqoga-Maunachira-Khwai subsystem and moderately underestimated in the Jao-Boro subsystem.

Simulated hydrographs indicate a flood wave travel time from upstream in the Panhandle to downstream in the delta in the order of 3 months, which largely corresponds to the general seasonal flood pattern observed in the delta. The simulated discharges are in most cases relatively close to the observed flow rates. The long term mean discharge appears to be simulated by the model but some displacement in time is seen in downstream stations. When comparing the values at individual gauging points it is important to stress the difference between model results representing the main channel and the flood plain, where observed discharges only cover the proportion of the flow within the main river cross section. Gauged values in sections of the river with flood plains where significant flow bypasses the gauging point are not directly comparable with simulated flow values .

For the calibration period, 1.1.2000–1.3.2004, the total ET losses of the delta almost exceed the rainfall and river discharge inputs (704mm). A storage decrease of 58mm is simulated by the model and the total flow across the downstream model boundary only amounts to 2mm, less than 1% of the inflow.

7.3 Model Application

Application of the ODMP Integrated Hydrologic Model in impact assessment and support of the management plan requires insight into the potential and the limitations. When interpreting model results in a management context it is important to be aware of the following limitations:

(1) Spatial scale - the model is developed at a 1km^2 grid resolution which by definition excludes the representation of any flow processes below this resolution. While simulating larger scale responses the model is not suited to the evaluation of detailed scale impacts.

(2) Temporal scale - the model has been tested and calibrated for a 4 year period, and some extreme events, eg years of exceptionally high or low inflows, are not represented. Due to both short term and long term changes in for example inflows and climate, the model has not been evaluated for the full range of flow conditions in recent decades.

(3) Calibration – observed data for calibration are limited in quantity and quality. When applying the model it is recommended to interpret model results as relative changes compared to a model simulated baseline or reference state.

7.4 Recommendations for Improvements

The ODMP Integrated Hydrologic Model may be improved as part of future work to enhance the operational use with the DWA Modelling Unit, supporting the model by additional data collection.

The model will be used by the DWA Modelling Unit to run scenarios and to analyse further the Okavango Delta hydrology. To improve the operational use of the model and to evaluate model performance, the run times should ideally be reduced and input data sets extended to facilitate simulation for decades representing significant climatic fluctuations. Model code optimisation will help increase the computational efficiency.

The density and continuity of available data are generally not sufficient for in-depth hydrologic analysis given the extent, complexity and dynamics of the Okavango Delta. Collection of field data as part of ongoing monitoring efforts is important to strengthen especially the calibration data sets. In particular the following data will help improve the ODMP hydrological model:

- Continuous climatic time series from within the delta (rainfall, relative humidity, temperature and solar radiation). A number of stations within the permanently and temporarily flooded areas will support rainfall inputs and simulation of ET rates. The use of stations close to the delta but in dry land areas may not fully represent internal Delta conditions

- River and channel cross sections for larger subsystems (Okavango, Nqoga, Maunachira, Khwai, Jao and Boro) with emphasis on flow split zones. Specific channel geometry and flood plain topography affects the separation of flow to subsystems and are thus crucial to simulation of changes in downstream conditions
- ET estimates for papyrus covered areas with varying water levels should be substantiated if suitable field data become available
- Assessment of simulated distributed ET rates by eg remote sensing techniques (results of ongoing PhD project) may be helpful in verifying the simulated, distributed ET rates
- The relationships between first of all flood and vegetation dynamics and secondly vegetation and ground water quality are not sufficiently documented or operational to include in the hydrologic model at the current stage. Scientific work to provide a closer description of such mechanisms in the Delta may enable incorporation in an integrated model in the future.

REFERENCES

/1/ GRAS, Topographic Model of the Okavango Delta, ODMP, Final Technical Report (2004)

/2/ McCarthy, T.S., Larkin, P.A., Bloem, A., 1998. Observations on the hydrology and geohydrology of the Okavango Delta. South African Journal of Geology, p. 101–117

/3/ Gumbricht T., Wolski P., Frost P., McCarthy T.S., Forecasting the spatial extent of the annual flood in the Okavango Delta, Botswana, Journal of Hydrology 290 (2004), p. 178–191

/4/ Timmermans W., Gieskea A., Wolski P., Arnethc A., Parodia G. Determination of Water and Heat Fluxes with MODIS imagery – Maun, Botswana. Journal of Hydrology

/5/ Water Resources Consultants for Department of Water Affairs, Botswana. Maun Groundwater Development Project – Phase 2, Resources Assessment and Well Field Development (2004)

/6/ McCarthy, J., Remote sensing for detection of landscape form and function of the Okavango Delta. PhD Thesis, Dep. of Land and Water Resources Engineering, Royal Institute of Technology, Stockholm (2002)

/7/ McCarthy, T.S., Cooper, G.R.J., Tyson, P.D. and Ellery, W.N., Seasonal Flooding in the Okavango Delta, Botswana - Recent History and Future Prospects. South African Journal of Science, (2000) vol.96, p. 25-33.

/8/ Bauer, P., Flooding and Salt Transport in the Okavango Delta, PhD thesis, Swiss Federal Institute of Technology, Zurich (2004)

/9/ Wolski, P (HOORC), Update of Conceptual Hydrological Model of the Delta, Water and Ecosystem Resources for Regional Development project, Deliverable D2.1 (2003)

/10/ Ringrose, S (HOORC), Ecology, Population Structure and Transboundary Movements of Elephants in the Okavango - Upper Zambezi Transfrontier Conservation Area (2002)

/11/ Kurugundla C.N., Mpho M., Kalaote K., Water Distribution and Losses with Special Reference to Blockages and Improved Monitoring in the Okavango Delta, Botswana, (2005). To be published.

/12/ MIKE SHE Technical Reference Manual, DHI, 2004

/13/ MIKE SHE Users Reference Manual, DHI, 2004

/14/ MIKE 11 Users Reference Manual, DHI, 2004

/15/ GRAS, Albedo and LAI Products from MODIS Satellite Data for the Okavango Delta Management Plan, Technical Report (2004)

APPENDIX 1 - SVAT MODEL

The SVAT component in MIKE SHE consists of a two source system (soil-canopy) linked by a network of resistances. The two layer model allows estimation of latent and sensible heat flux from canopy to mean source (LEc, Hc), soil to mean source (LEs, Hs), and mean source to atmosphere (LEa, Ha) separately. Furthermore, the scheme distinguishes evaporation from the substrate and ponded water on the surface (LEds and LEws, respectively) as well as transpiration and evaporation from the wet part of the canopy (LEdc and LEwc, respectively). Adopting the resistance analogy, the fluxes of latent and sensible heat between nodes are driven by differences in humidity and temperature, respectively, and controlled by a number of resistances. The resistances depend on the internal state of the land-surface-vegetation system as well as the atmospheric conditions. The model structure is illustrated in Figure A1.1.

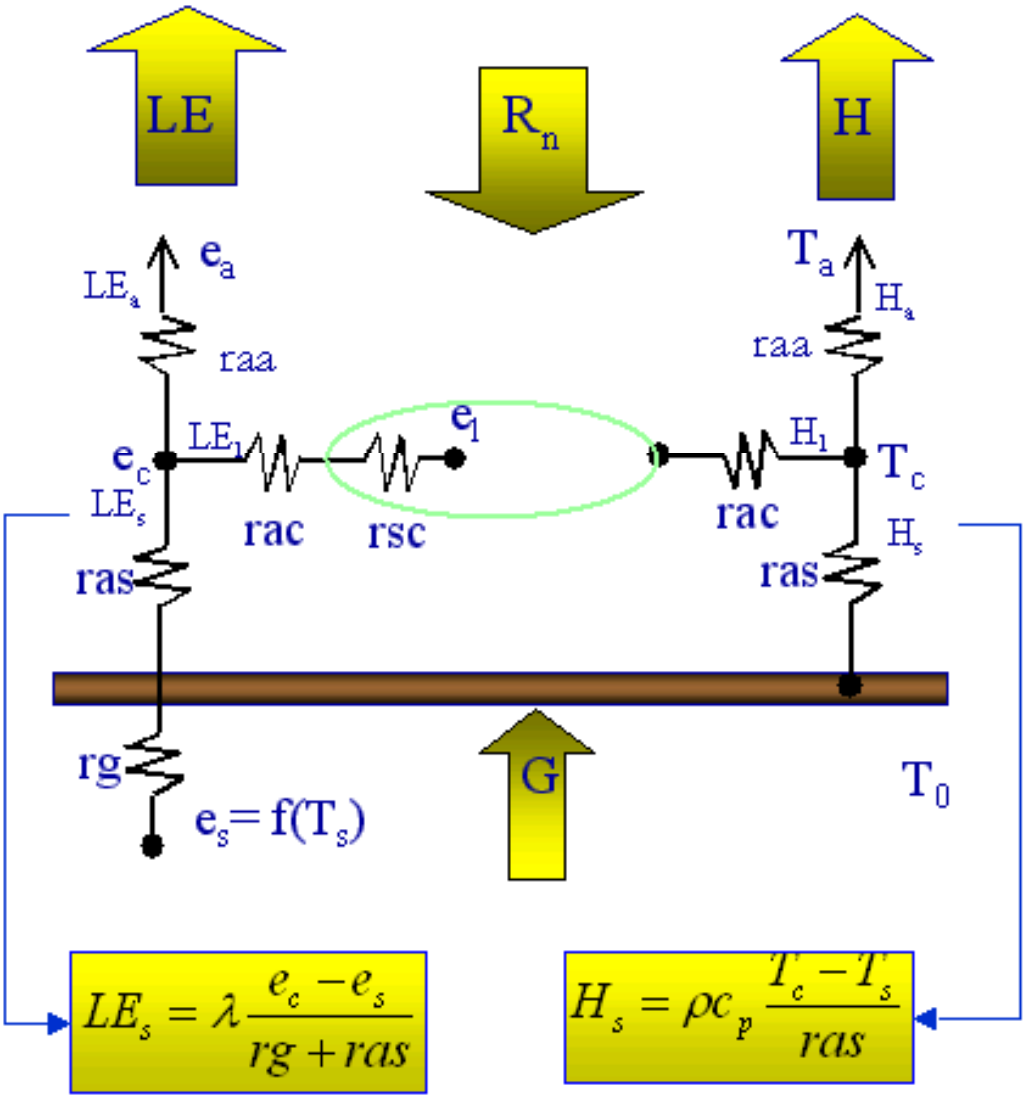

Figure A1.1: SVAT Model Structure

Climate Input

The model is driven by prescribed climate observations. Air temperature (T_a), air-humidity (e_a), wind speed (w_a), incoming short-wave radiation (SW_{in}) and air pressure (P) are usually available, but incoming long wave radiation is usually not measured, and to require this to be

specified would limit the practical use of the model significantly. Instead the long wave radiation is calculated internally, based on the prescribed incoming short wave radiation and air humidity. In each time step, the specified incoming short wave radiation is compared to the amount of radiation that would reach the land surface under clear sky conditions (derived in Appendix A.2), and this ratio is used to calculate the cloudiness (C) according to the Prescott formula:

$$C = \frac{\frac{SW_{in}}{SW_{clear}} - 0.21}{0.5} \qquad (1)$$

Once the cloudiness is known, emissivity of the atmosphere is calculated according to Croley (1989)

$$\varepsilon_a = \left(0.53 + 0.00065\sqrt{e_a}\right)\left(1 + 0.40C\right) \quad (2)$$

and finally incoming long-wave radiation is calculated using Boltzmans law:

$$LW_{in} = o\varepsilon_a T_a^4$$

Sensible and Latent Heat Fluxes

In generic form, the sensible and latent heat fluxes between two nodes in the resistance network can be written according to equations (1) and (2):

$$H_{12} = \rho c_p \frac{T_2 - T_1}{r_{12}} \qquad (1)$$

$$LE_{12} = \rho c_p \frac{e_2 - e_1}{r_{12}} \qquad (2)$$

T is the temperature [K] and *e* is the absolute humidity of the air [kg/m3]. Based on this analogy the fluxes between the nodes can be expressed through the following 10 equations:

$$H_a = \rho c_p \frac{T_c - T_a}{r_a^a} \quad ; \quad LE_a = \lambda \frac{e_c - e_a}{r_a^a} \qquad (3+4)$$

$$H_s^w = \rho c_p \frac{T_s^w - T_c}{r_a^s} \quad ; \quad LE_s = \lambda \frac{e_s^w - e_c}{r_a^s} \qquad (5+6)$$

$$H_s^d = \rho c_p \frac{T_s^d - T_c}{r_a^s} \quad ; \quad LE_s^d = \lambda \frac{e_s^d - e_c}{r_a^s + r_g} \qquad (7+8)$$

$$H_c^w = \rho c_p \frac{T_l^w - T_c}{r_a^c} \quad ; \quad LE_c^w = \lambda \frac{e_l^w - e_c}{r_a^c} \qquad (9+10)$$

$$H_c^d = \rho c_p \frac{T_l^d - T_c}{r_a^c} \quad ; \quad LE_c^d = \lambda \frac{e_l^d - e_c}{r_a^c + r_s^c} \qquad (11+12)$$

Equation 3-12 contains the following ten unknowns:

$$T_s^d, T_s^w, T_c, T_l^d, T_s^w, e_s^d, e_s^w, e_c, e_l^d, e_s^w$$

Hence, five resistances ($r_a^a, r_a^s, r_a^c, r_s^c, r_g$) need to be parameterised and ten independent equations need to be derived to solve for the fluxes of heat and water.

Resistances

The fluxes between the nodes in the network are controlled by five resistances. The formulations used for each resistance is described in this section.

Aerodynamic Resistance

The aerodynamic resistance expresses the ability of the air to transport energy and water away from the canopy. It depends on the degree of turbulence above the canopy and consequently on the stability of the atmosphere. If the surface is warmer than the air masses above (ie unstable conditions), buoyancy will significantly increase the upward heat and water transport. Under stable conditions the aerodynamic resistance increases due to the stable stratification of the atmosphere. The aerodynamic resistance is expressed according to Mahrt and Ek (1996). This approach is based on the Richardson number (R) and a stability number (F):

$$r_a^a = \frac{\log\left(\frac{z_{ref} - z_d}{z_0^m}\right)\log\left(\frac{z_{ref} - z_d}{z_0^h}\right)}{\kappa^2 w_s}\frac{1}{F}$$

where z_{ref} and z_d is the measuring height and displacement height, respectively. z_0^m and z_0^h is the roughness length for momentum and heat, respectively. κ is the von Karman Constant and u_{ref} is the wind speed at reference height. Richardson's number is calculated as:

$$Ri = \frac{g}{T_a}\frac{(T_a - T_c)(z_{ref} - z_d)}{u_{ref}^2}$$

The equation for the stability factor (F) depends on whether the atmosphere is stable or not:

R<0 (unstable)

$$F = 1 - 0.15\frac{Ri}{1 + 0.75\kappa^2\sqrt{-Ri\frac{z_{ref} - z_d}{z_o^m}}\Big/\left(\log\frac{z_{ref} - z_d}{z0m}\log\frac{z_{ref} - z_d}{z0h}\right)}$$

R>0 (stable)

$$F = \exp(Ri)$$

Resistance between Soil Surface and Mean Source

Resistance between soil surface and canopy air is parameterised as proposed by (Choudhury and Monteith, 1988).

$$r_a^s = \frac{h_{veg}\exp(\alpha_k)}{\alpha_k K_e}\left(\exp\left(-\alpha_k z_0^s \Big/ h_{veg}\right) - \exp\left(-\alpha_k (z_0 - z_d) \Big/ h_{veg}\right)\right)$$

where α_k is the attenuation coefficient of eddy diffusivity through sparse canopy. Normally the value is in the range 2.0 – 2.5 (Daamen, 1997; Choudhury and Monteith, 1988;Shuttleworth and Gurney, 1990). K(h) is the eddy diffusion coefficient defined as:

$$K_e = \frac{\kappa^2 u_{ref}\left(h_{veg} - z_d\right)}{\ln\left(\frac{z_{ref} - z_d}{z_0}\right)}$$

Resistance between Leaves and Mean Source

The leaf boundary layer resistance (r_a^c) is parameterised according to Choudhury and Monteith (1988):

$$r_a^c = \frac{\alpha_u}{2 \cdot a \cdot LAI}\left(\frac{w}{u_h}\right)^{0.5} \frac{1}{1 - \exp\left(-0.5\alpha_u\right)}$$

where a is a constant and w is the average leaf width and u_h is the wind speed at the top of the canopy. Daamen, (1997) uses a = 0.00662.

Stomata Resistance

The stomata resistance is parameterised using a Jarvis-type model (Jarvis, 1976; Stewart and Gay, 1988)

$$r_s^c = \frac{r_{s,\min}^c}{LAI \cdot F1 \cdot F2 \cdot F3 \cdot F4}$$

The reduction functions, F1–F4, represent the influence of radiation, temperature, air humidity and soil moisture on the stomata resistance. The unstressed stomatal resistance, $r_{s,\min}^c$, is normally found in the range 40 s/m - 140 s/m (Kelliher et al., 1995).

The reduction function for global radiation is parameterised as proposed by (Dickinson, 1984):

$$F1 = \frac{\frac{r_{s,\min}^c}{r_{s,\max}^c} + 0.0055\frac{2S_i}{LAI}}{1 + 0.0055\frac{2S_i}{LAI}}$$

The stomata resistance tends to increase as the leaf-to-air humidity difference increases. This is parameterised according to Verma et al. (19XX):

$$F2 = \left(1 + \varsigma\left(e_{a,sat} - e_a\right)\right)^{-1}$$

where $\varsigma = 0.57 m^3 / kg$.

The stomata resistance increases when the leaf-to-air temperature difference increases and this is parameterised according to Jarvis (1976).

$$F3 = 1 - \xi\left(T_{ref} - T_a\right)^2$$

where T_{ref} is a reference temperature set to 298K by Dickinson (1984).

Finally, the influence of soil moisture on transpiration has to be taken into consideration. In MIKE SHE, a simple linear expression is used to relate the available soil moisture to the soil moisture reduction function. The reduction function is calculated by weighting a root density function with the available soil moisture content.

$$F4 = \sum_{j=1}^{M} RDF_j \frac{\theta_j - \theta_{w,j}}{\theta_{fc,j} - \theta_{w,j}}$$

where θ_w and θ_{fc} is the soil moisture content at wilting point and field capacity. M is the number of computational layers containing roots. The root density function for layer j is calculated as:

$$RDF_j = \frac{\int_{z_j}^{z_{j+1}} N(z)dz}{\int_0^{z_{rd}} N(z)dz}$$

where z_j and z_{j+1} are the top and bottom depths of layer j, z_{rd} is the root depth and N(z) is root length per vertical depth, at depth z. N(z) is approximated with a logarithmic expression.

Resistance to Soil Evaporation

As the soil dries out, the resistance to soil evaporation increases. The formulation proposed by Sellers et al. (1992) is used here:

$$r_g = \exp\left(8.206 - 4.255 \frac{\theta - \theta_{wp}}{\theta_{sat} - \theta_{wp}}\right)$$

where θ is the soil moisture content of the uppermost computational node in the unsaturated zone.

Soil Heat Flux, G

In sparse canopies the soil heat transfer can have a significant influence on the energy availability at the soil surface (references). In MIKE SHE the transport of heat in the soil is based on the one-dimensional heat transfer equation:

$$G = -K_h \frac{\partial T}{\partial z}$$

Solution Scheme

If the wet fraction of the soil surface and canopy are denoted w_s and w_c, respectively, the total fluxes from the canopy and substrate to the mean source are written:

$$LE_s = w_s LE_s^w + (1 - w_s) LE_s^d \qquad (13)$$

$$LE_c = w_c LE_c^w + (1 - w_c) LE_c^d \qquad (14)$$

$$H_s = w_s H_s^w + (1 - w_s) H_s^d \qquad (15)$$

$$H_c = w_c H_c^w + (1 - w_c) H_c^d \qquad (16)$$

where LE and H are in W/m^2. Two independent equations are obtained by expressing the total latent and sensible heat flux by equations 13-16:

$$LE_a = w_s LE_s^w + (1-w_s)LE_s^d + w_c LE_c^w + (1-w_c)LE_c^d \qquad (17)$$

$$H_a = w_s H_s^w + (1-w_s)H_s^d + w_c H_c^w + (1-w_c)H_c^d \qquad (18)$$

Energy conservation at the dry part of the soil and canopy surface yield two more equations:

$$(1-w_s)R_{ns} = (1-w_s)H_s^d + (1-w_s)H_s^d + (1-w_s)LE_s^d + (1-w_s)G_s^d \qquad (19)$$

$$(1-w_c)R_{nc} = (1-w_c)H_c^d + (1-w_c)H_c^d + (1-w_c)LE_c^d \qquad (20)$$

Similar energy balances can be written for the wet part of the soil and canopy:

$$w_s R_{ns} = w_s H_s^w + w_s LE_s^w + w_s G_s^w \qquad (21)$$

$$w_c R_{nc} = w_c H_c^w + w_c LE_c^w \qquad (22)$$

Soil heat flux (G) is calculated based on the one-dimensional heat transfer equation:

$$G = -K_h \frac{\partial T}{\partial z} \qquad (23)$$

Net radiation is calculated using Boltzman's Law, and depends on the temperature in the canopy and on the surface of the substrate. The net radiation above the canopy is calculated as:

$$R_n = LW_{net} + SW_{net} = SW_{in}(1-\alpha) + \sigma\left(\varepsilon_a T_a^4 - \varepsilon_s T_r^4\right)$$

T_r is the radiometric surface temperature which is calculated according to Normal et al. (1995):

$$T_r = \left[f(LAI) * T_{l,eff}^4 + (1-f(LAI))T_{s,eff}^4\right]^{1/4}$$

where f(LAI) is the fraction of the model grid covered by vegetation. Here, a simple exponential function is used:

$$f(LAI) = 1 - \exp\left(-k_{ext} \cdot LAI\right)$$

where the extinction coefficient K_{ext} is usually found in the range 0.3 – 0.5. The net radiation is divided between the canopy and vegetation according to $f(LAI)$:

$$R_{ns} = R_n\left(1 - f(LAI)\right)$$

$$R_{nc} = R_n f(LAI)$$

The last four equations required solving for the unknown temperatures and humidities. These are obtained by relating the humidity at the wet and dry part of the soil surface, in the plant stomata and at the wet leaf surface to the respective temperatures. For the humidity at the wet part of the soil surface, the wet part of the canopy as well as inside the plant stomata it seems reasonable to assume saturation humidity corresponding to T_s^w, T_l^w and T_l^d, respectively. Regarding the calculation of soil evaporation from the dry part of the soil surface, a more conceptual approach is selected by which the humidity is assumed to be at saturation at all times, and let the soil evaporation resistance, r_g, act as the soil moisture reduction function. This approach allows us to express the humidity at the dry part of the soil

surface as a function of T_s^d only. Hence, e_s^d, e_s^d, e_l^d and e_l^w can be expressed as function of the temperatures T_s^d, T_s^w, T_l^d and T_l^w by using the following empirical relationship:

$$e_X^Y = 611Pa \cdot \exp\left(17.27 \frac{T_X^Y}{T_X^Y + 237.3^\circ C}\right), \qquad X = s,l \qquad and \qquad Y = w,d$$

Equation 17-2, now constitutes ten equations in ten unknowns: $T_s^d, T_s^w, T_c, T_l^d, T_s^w, e_s^d, e_s^w, e_c, e_l^d, e_s^w$. Solving for these unknowns and inserting in equation 3-12 the fluxes of heat and water can be determined. Due to the non-linear behaviour of some of the resistances the system of equations will be highly non-linear. Solution of the full, non-linear system would be computationally demanding, and keeping in mind that the model is implemented in a distributed model, not suitable. Instead, a less computationally demanding method is selected, where the temperatures and humidities listed are calculated implicitly, but the coefficients in the resulting matrix equation are calculated explicit, is adopted (eg Kamitsas). This implies that previous time-step temperatures and humidities are used to calculate resistances, and that previous time step values are used to calculate net-radiation. Moreover, the non-linear expression used to calculate the saturation humidity as a function of temperature is replaced by its truncated expansion:

$$e_{x,sat}(T_X^{t+1}) = e_{X,sat}\left(T_X^t\right) + \left.\frac{\partial e_{x,sat}}{\partial T_X}\right|_{T_X^t} \left(T_X^{t+1} - T_X^t\right), \qquad X = l,s$$

This allows us to establish a system consisting of ten linear equations in ten unknowns ($T_s^d, T_s^w, T_c, T_l^d, T_s^w, e_s^d, e_s^w, e_c, e_l^d, e_s^w$). The solution of this system is much faster than solving the original non-linear system of equations.

Ten equations in ten unknowns ($T_s^d, T_s^w, T_c, T_l^d, T_s^w, e_s^d, e_s^w, e_c, e_l^d, e_s^w$) have to be solved in every time step. After combining the equations and rearranging the terms, the following ten equations are derived:

$$\underline{LE_a = w_s LE_s^w + (1-w_s)LE_s^d + w_c LE_c^w + (1-w_c)LE_c^d}:$$

$$\underbrace{\frac{1-w_s}{r_g + r_a^s}}_{a1-6} e_{sd}^{t+1} + \underbrace{\frac{w_s}{r_a^s}}_{a1-7} e_{sw}^{t+1} \underbrace{- \left(\frac{1-w_s}{r_g + r_a^s} + \frac{w_s}{r_a^s} + \frac{1-w_l}{r_a^c + r_s^c} + \frac{w_l}{r_a^c} + \frac{1}{r_a^a}\right)}_{a1-8} e_c^{t+1} + \underbrace{\frac{1-w_l}{r_a^c + r_s^c}}_{a1-9} e_{ld}^{t+1} + \underbrace{\frac{w_l}{r_a^c}}_{a1-10} e_{lw}^{t+1} = \underbrace{-\frac{1}{r_a^a} e_a^{t+1}}_{b1}$$

$$\underline{H_a = w_s H_s^w + (1-w_s)H_s^d + w_c H_c^w + (1-w_c)H_c^d}:$$

$$\underbrace{\frac{1-w_s}{r_a^s}}_{a2-1} T_{sd}^{t+1} + \underbrace{\frac{w_s}{r_a^s}}_{a2-2} T_{sw}^{t+1} \underbrace{- \left(\frac{1-w_s}{r_a^s} + \frac{w_s}{r_a^s} + \frac{1-w_l}{r_a^c} + \frac{w_l}{r_a^c} + \frac{1}{r_a^a}\right)}_{a2-3} T_c^{t+1} + \underbrace{\frac{1-w_l}{r_a^c}}_{a2-4} T_{ld}^{t+1} + \underbrace{\frac{w_l}{r_a^c}}_{a2-5} T_{lw}^{t+1} = \underbrace{-\frac{1}{r_a^a} T_a^{t+1}}_{b2}$$

$$\underline{w_s R_{ns} = w_s H_s^w + w_s LE_s^w + w_s G_s^w}$$

$$\underbrace{\left(\rho c_p \frac{1}{r_a^s} + \frac{K_h}{\Delta z_N}\right)}_{a3-2} T_{sw}^{t+1} \underbrace{- \rho c_p \frac{1}{r_a^s}}_{a3-3} T_c^{t+1} + \underbrace{\lambda \frac{1}{r_a^s}}_{a3-7} e_{sw}^{t+1} \underbrace{- \lambda \frac{1}{r_a^s}}_{a3-8} e_c^{t+1} = \underbrace{R_{ns}^t + K_n \frac{T_{s,N}}{\Delta z_N}}_{b3}$$

$$\underline{(1-w_s)R_{ns} = (1-w_s)H_s^d + (1-w_s)H_s^d + (1-w_s)LE_s^d + (1-w_s)G_s^d}$$

$$\underbrace{\left(\rho c_p \frac{1}{r_a^s} + \frac{K_h}{\Delta z_N}\right)}_{a4-1} T_{sd}^{t+1} \underbrace{- \rho c_p \frac{1}{r_a^s}}_{a4-3} T_c^{t+1} + \underbrace{\lambda \frac{1}{r_a^s + r_g}}_{a4-6} e_{sd}^{t+1} \underbrace{- \lambda \frac{1}{r_a^s + r_g}}_{a4-8} e_c^{t+1} = \underbrace{R_{ns}^t + K_n \frac{T_{s,N}}{\Delta z_N}}_{b4}$$

$$\underline{(1-w_c)R_{nc} = (1-w_c)H_c^d + (1-w_c)LE_c^d :}$$

$$\underbrace{- \rho c_p \frac{1}{r_a^c}}_{a5-3} T_c^{t+1} + \underbrace{\rho c_p \frac{1}{r_a^c}}_{a5-4} T_{ld}^{t+1} \underbrace{- \lambda \frac{1}{r_a^c + r_s^c}}_{a5-8} e_c^{t+1} + \underbrace{\lambda \frac{1}{r_a^c + r_s^c}}_{a5-9} e_{ld}^{t+1} = \underbrace{R_{nc}}_{b5}$$

$$w_c R_{nc} = w_c H_c^w + w_c LE_c^w$$

$$\underbrace{- \rho c_p \frac{1}{r_a^c}}_{a6-3} T_c^{t+1} + \underbrace{\rho c_p \frac{1}{r_a^c}}_{a6-5} T_{lw}^{t+1} \underbrace{- \lambda \frac{1}{r_a^c}}_{a6-8} e_c^{t+1} + \underbrace{\lambda \frac{1}{r_a^c}}_{a6-10} e_{lw}^{t+1} = \underbrace{R_{nc}}_{b6}$$

$$e_{lw}^{t+1} = e_a^{t+1} + \Delta\left(T_{lw}^{t+1} - T_a^{t+1}\right)$$

$$\underbrace{\Delta}_{a7-5} \cdot T_{lw}^{t+1} \underbrace{-1}_{a7-10} \cdot e_{lw}^{t+1} = \underbrace{\Delta \cdot T_a^{t+1} - e_a^{t+1}}_{b7}$$

$$\underline{e_{ld}^{t+1} = e_a^{t+1} + \Delta\left(T_{ld}^{t+1} - T_a^{t+1}\right)}$$

$$\underbrace{\Delta}_{a8-4} \cdot T_{ld}^{t+1} \underbrace{-1}_{a8-9} \cdot e_{ld}^{t+1} = \underbrace{\Delta \cdot T_a^{t+1} - e_a^{t+1}}_{b8}$$

$$\underline{e_{sw}^{t+1} = e_a^{t+1} + \Delta\left(T_{sw}^{t+1} - T_a^{t+1}\right)}$$

$$\underbrace{\Delta}_{a9-2} \cdot T_{sw}^{t+1} \underbrace{-1}_{a9-7} \cdot e_{sw}^{t+1} = \underbrace{\Delta \cdot T_a^{t+1} - e_a^{t+1}}_{b8}$$

$$\underline{e_{sd}^{t+1} = e_a^{t+1} + \Delta\left(T_{sd}^{t+1} - T_a^{t+1}\right)}$$

$$\underbrace{\Delta}_{a10-1} \cdot T_{sd}^{t+1} \underbrace{-1}_{a10-6} \cdot e_{sd}^{t+1} = \underbrace{\Delta \cdot T_a^{t+1} - e_a^{t+1}}_{b10}$$

APPENDIX 2 – CLEAR SKY SHORT WAVE RADIATION

The incoming short wave radiation (SW_{clear}) during any given day at time t (0<t<24) is calculated in every time step as:

$$SW_{clear} = \max\left[0; I_{sc} E_0 \left(\sin\Lambda \sin\delta + \cos\Lambda \cos\delta \cos\left(\omega\left(t - T_s\right)\right)\right)\right]$$

Here, I_{sc} is the solar constant, E_0 is the eccentricity correction factor, Λ is the latitude, δ is the declination of the sun, T_s is the time of true solar noon, and ω is the angular velocity of the Earths orbit around the Earth (ω=2.0e-7 rad/s). Each term is explained in the following. Notice that the formulation breaks down during night time, where the incoming short wave radiation is set to zero.

Solar Constant

The solar constant describes the average quantity of solar radiation received by a horizontal surface located right outside of the Earth's atmosphere. This value is approximately 1,370 watts per square meter.

Eccentricity Correction Factor

During the annual orbit around the sun, the distance between the Sun and Earth changes regularly, as expressed by the eccentricity correction factor (E_0). To calculate E_0, the model has to keep track of the position of the Earth relative to the Sun. This position is expressed by the day-angle (Γ):

$$\Gamma = \frac{2\pi}{365}(J - 1)$$

where J is the Julian day number. The eccentricity factor, defined as the square of the ratio of the average distance (r_0) relative to the distance at a given time (r), can now be calculated from the day-angle:

$$E_0 = \left(\frac{r_0}{r}\right)^2 = 1.000110 + 0.034221\cos\Gamma + 0.001280\sin\Gamma + 0.000719\cos 2\Gamma + 0.000077\sin 2\Gamma$$

Declination

The declination is defined as the latitude at which the sun is directly overhead. Due to the tilt of the Earths rotational axis this latitude changes regularly during the year. The declination is calculated as:

$$\begin{aligned}\delta = {} & 0.0006918 - 0.399912\cos\Gamma + 0.070257\sin\Gamma \\ & - 0.006758\cos 2\Gamma + 0.000307\sin 2\Gamma \\ & - 0.002697\cos 3\Gamma + 0.00148\sin 3\Gamma\end{aligned}$$

Time of True Solar Noon

True solar noon is defined as the point of time when the sun is aligned with true south or true north. Due to the Earth's tilt and elliptical orbit, the true solar noon does not normally coincide with noon (t=12h). The difference between noon and the true solar noon is expressed by the Equation of Time (EOT):

$$EOT = \frac{9.87 \sin 2B - 7.53 \cos B - 1.5 \sin B}{60}$$

B is defined as:

$$B = \frac{J - 81}{364} 2\pi$$

Now the time of true solar noon can be calculates as $T_s = 12h + EOT$.

APPENDIX 3 - MORPHOLOGY AND SEDIMENT TRANSPORT IN OKAVANGO DELTA

INTRODUCTION

The present note is a working paper on the Morphology and Sediment Transport of the Okavango Delta. The paper provides an overview of the planned study.

Stakeholder Concerns

A workshop held by the ODMP Hydrology Component and attended by representatives of most of the other components in February 2005 gave some ideas about the main stakeholder concerns and interests related to morphology and sediment transport:

- Shift of major channels from eg one side of the delta to the other, which will have a major impact for a number of stakeholders (large scale morphology)
- Impact of river basin development in the upper catchment on the ecosystem, including the impact of any future reservoirs
- Blockage of channels causing dry rivers further downstream; alternative distribution locally between channel flow and overland flow (small scale morphology)
- Fine, organic-rich sediment being washed into the river causing oxygen depletion, and which has an impact on fish.

Although related to morphology and sediment transport, the latter (oxygen depletion by SOD) is not part of the present scope of work. It should be linked to a water quality study component.

Physical Characteristics

Following a review of previous research work described in various papers, a summary of the key characteristics has been prepared in the following sections. Briefly they are:

- In the long term, shifts in distributary channels with a time scale of 50-100 years induced by sedimentation (of bed load) and tectonic activity. Major shifts in the past have caused significant local changes and induced increased diversity of habitats.
- In the short term, large spatial and temporal variations in sedimentation areas, and sediment distribution in channel splits. Sediment transport occurs especially in the Panhandle, where the majority of the bedload deposits in the dry season.
- Unique channel and flood plain interaction with seepage and overspill through the vegetation-flanked channels to the flood plain causing velocity decrease, bed aggradation, vegetation growth and eventually decline of the channel. Hippopotami maintain pathways in back swamp areas, which may lead to new channel systems through channel avulsion.

- Channel avulsion, which diverts all or part of the discharge of a river to a lower part of the adjacent flood plain to form a new channel. This water will be free of sediment as it passes through "filters" of vegetation along the channel banks. By headward propagation, the secondary channel may ultimately connect back to the main channel.

- Former intervention measures through dredging and excavation in the lower Boro (in the 1970s) have improved outflow of water and navigability but also caused adverse effects on adjacent flood plain habitats.

A few sediment data are available from the research work by the research group in the University of Witwatersrand, Johannesburg. The data are described in the reviewed papers.

Channel Dynamics

The network of channels in the Okavango Delta is divided into primary channels and secondary channels. The channels are constantly shifting with a time scale of the order of 50 to 100 years. Examples: Thaoge River was blocked in 1880s; lower reach of Nqoga blocked in 1920s; the Boro River system was activated in 1952 following a major earthquake. A combination of sedimentation and tectonic activity cause channel failure.

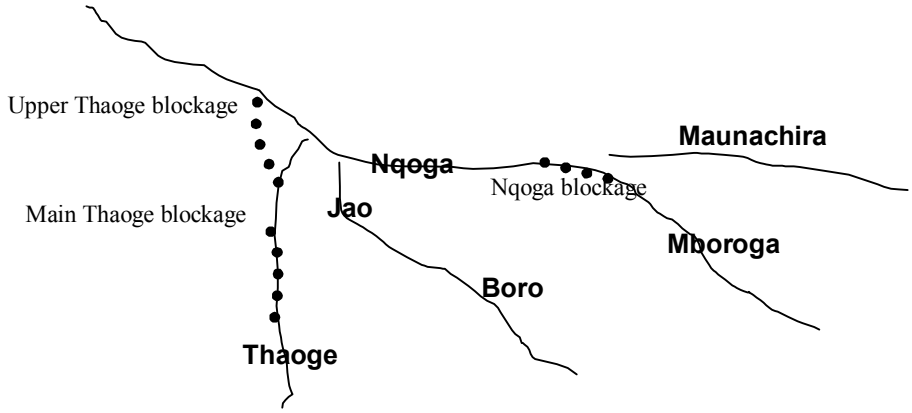

Sedimentation (overall)

Sedimentation is a combination of clastic sedimentation (170,000t bed load and 39,000t suspended load per year) on the upper fan and chemical sedimentation (381,000t dissolved load per year) on the lower fan. The channels are important arteries for distributing not only water but also sediment to the fan. Bed load can only be transported in the primary channels, whereas suspended and dissolved load is transported through channel as well as overland flow. All bed load and suspended load is trapped in the delta. Bed load is responsible for channel aggradation and eventual blockage. Suspended load is trapped in the adjacent swamps.

Tectonic Activity

Crustal instability and neotectonic activity appears to be important. Because of low topographic gradients, small earth movements are capable of inducing large scale changes in the distribution of water. The area is a tectonically active extension of the East African Rift system. As described above, the earthquake in 1952 caused some redistribution of flow patterns in the area, for instance the Boro flow system, which became active.

Sediment Transport Characteristics

The bed load is a highly non-linear function of the flow velocity. Thus, the majority of all bed load over a year is imported to the delta during the flood season. 90% of the bedload deposits in the Panhandle during the low flow season. Extreme flood events move the sediment further downstream. Sediment accumulates in a non-uniform pattern in the delta area.

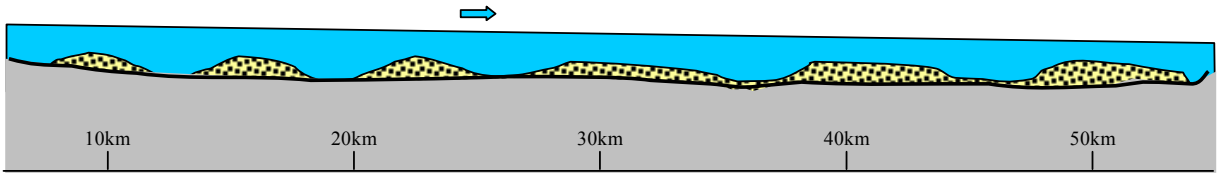

Some depositional areas during low flow conditions may turn into erosion areas in high flow conditions. Examples are meander bends characterised by bend scour along the outer bank. Thus, inflow of sediment to the delta can be considered as "waves" of sediment propagating downstream. Channel blockage, channel avulsion as well as extreme flood events will induce new waves of sandy sediment in the channel system.

Sediment Distribution in Channel Bifurcations

Spill and seepage of water from a primary channel to a secondary channel which is separated by a "filter" of vegetation and peat does not allow bedload transport of sediment from the primary to the secondary channel. Thus, all bedload is trapped in the main channel. In a flow split, the sediment is not necessarily distributed proportionally to the flow distribution. The distribution of bedload between two downstream channels depends on the local planform as well as the history of flow events at the flow split. Often, a sandbar is building up in front of a small distributary during high flow, and eroding during low flow. Thus, although the shape of the offtake from the main channel (the angle) appears unfavourable for sediment import, substantial bedload may still be conveyed into the distributary.

Channel and Flood Plain Interaction

Overspill from the channels and sheet flow are responsible for water dispersal in the delta. Channel margins are formed by peat, stabilised by vegetation, which allow water to leak from the channels. The loss of water to the adjacent swamp areas and the reduction in flow discharge causes loss of sediment transport capacity and subsequent sedimentation. The deposition of the sandy bedload material leads to aggradation of the channel bed. Elevated channels cause additional leakage of water from the channel through the flanking vegetation as the transverse water gradient increases and the longitudinal water gradient decreases. The balance between water loss, sediment transport and channel aggradation changes depending on the water level stage (low flow or high flow conditions).

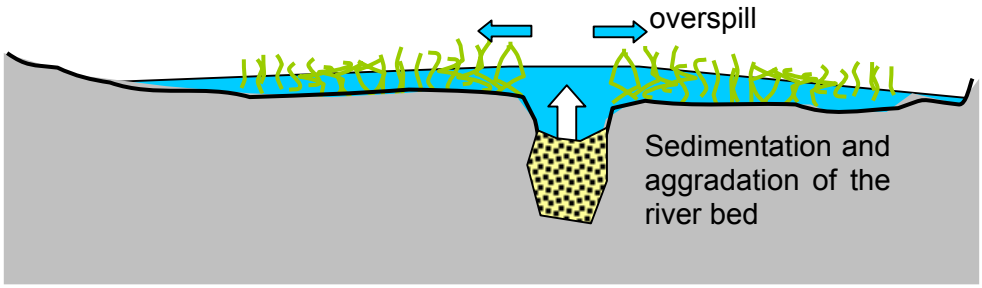

Flow and Bedload Capacity of Channel

The shape of the channel cross section and the downstream gradient provide a given flow and thereby sediment transport capacity. As the water level increases during the flood season, more and more water is transported as overland flow and sheet flow, and the percentage of total flow in the channel decreases. Thus, if the total inflow at Mohembo increases by for instance 100%, the in-channel flow further downstream may not increase by more than say 20%.

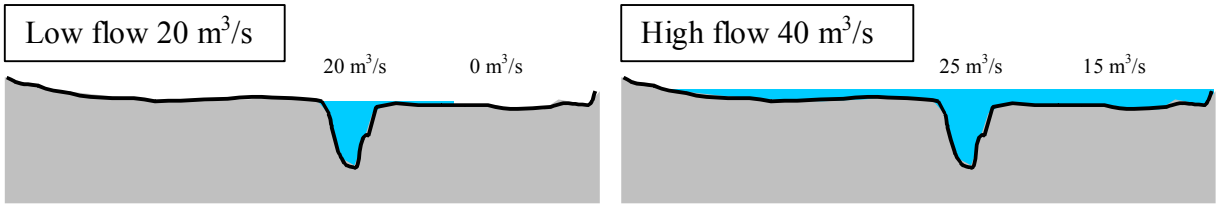

Channel Avulsion

An avulsion diverts all or part of the discharge of a river (primary channel) to a lower part of the adjacent flood plain to form a new channel (secondary channel). This water will be free of sediment as it passes through "filters" of vegetation along the channel banks. The Maunachira River is an example of a secondary channel which developed following closure of the lower reach of the Nqoga. Thus, avulsion takes place following accumulation of sediment in the parent channel. Seismic earth movement may further enhance avulsion.

Vegetation and Morphology

There is a balance between flow velocity, depth, and growth and type of vegetation. Thus, as the channel flow velocity starts to decline, the closure of the channel is further enhanced by encroachment of vegetation, especially papyrus, into the river. Decline in current velocity is the main cause of channel decline. From research studies there are no indications, however, that vegetation growth or debris flow is the main factor responsible for initiation of channel closure. It is an indication of channel closure and it accelerates the process once it is started. Vegetation further makes the channels highly resistant to bank erosion.

Hippopotamus

Research studies have suggested that hippopotami have a catalytic effect on geomorphological changes. Firstly, hippopotami maintain pathways in back swamp areas which allow rapid distribution of water and leading to a new channel system through avulsion. Secondly, hippopotami create breaches in the vegetation levees, which flank the channels in the permanent swamps. The network of hippopotamus trails adjacent to channels provides lines of potential weakness.

Erosion of Secondary Channels

Secondary channels, which are products of channel avulsion, are not directly connected to the external source of sediment (the Okavango River). If the flow in a secondary channel is sufficient to generate sediment transport (bedload), and there is no upstream supply, erosion in the upstream reach of the secondary channel will inevitably take place. The channel will propagate headwards. With erosion upstream and deposition downstream, the slope will gradually decrease in the secondary channel. By headward propagation, the secondary channel may ultimately connect back to the main channel.

Dredging Interventions

Dredging in the lower reaches in the 1970s (straightening of channels) resulted in decreased stability of the channel bed and drying out of the flood plain. Dredging created a nick point (break in slope) which has been migrating upstream by headward erosion since dredging ceased.

STUDY OBJECTIVES

Scope

To study the influence of the development of storage in the upper catchment, it is proposed to use the channel surface component (MIKE 11) of the integrated hydrologic model described in the main report. MIKE 11 includes a sediment transport module which can simulate the transport of bedload and the impact on the river morphology in terms of aggradation and degradation. This model will not be able to provide a detailed prediction of the long term development of the morphology (eg development of alignment of river geometry – no model can do that), but it will predict trends and time scales for the morphological developments and how the impact of interventions in the catchment.

The output is defined as follows in the proposal:

- Screening of user needs and data availability related to sediment transport and morphology
- Agreed model specifications.
- An operational and well documented comprehensive integrated model (jointly with other specialists under the overall responsibility of the team leader).
- Trained Staff

In addition, the DWA Modelling Unit will carry out sediment transport study activities.

Output

Based on the defined scope, the Consultants' proposal, the interpretation of prevailing physical characteristics from the review of previous research work (University of Witwatersrand), the initial feedback from stakeholders, as well as the allocated resources, the following immediate objectives are defined.

- Recommendations on a monitoring programme for morphology and sediment transport, first of all the routine measurements at Mohembo Gauging Station.
- A sediment model will be prepared for future management and decision support related to large scale and long term morphology with the shift of major channels from eg one side of the delta to the other, which will have big impact for a number of stakeholders. An example of the investigation of the impact of upstream catchment changes using the tool will be provided.
- Provide understanding of the small scale morphology with blockage of channels causing dry rivers further downstream, alternative distribution locally between channel flow and overland flow and impact of dredging and similar intervention measures. The same tool as above can be used for management and decision support
- Training of the modelling unit in using the sediment sub-model together with the integrated ground-surface water hydrologic model

Analyses of the impact of vegetation on river morphology from a time series of satellite images as specified in the proposal will not be carried out for two reasons. Firstly, no such time series of detailed satellite images is available at the same time as information about channel decline (discharge data or geometry data). Secondly, McCarthy et al showed in their research work that vegetation growth and encroachment into the channel is a symptom rather than a cause of beginning channel decline.

METHODOLOGY

Monitoring Programme

The Recommendations for Improved Hydrologic Monitoring in the Okavango Delta are being refined with respect to sediment transport, in particular the introduction of sediment transport monitoring at the Mohembo Gauging Station, a cooperation between DWA and HOORC.

Review of Literature

A study and interpretation of previous work, especially by the Okavango Research Group in the University of Witwatersrand, Johannesburg, headed by Prof TS McCarthy has been prepared. Since 1984, the group has generated a significant amount of high quality research results, which are very valuable for the sediment sub-component. A summary of reviewed papers and reports related to sediment in Okavango has been prepared.

Data Processing and Interpretation

Some sediment data are available from the research work by the research group in University of Witwatersrand, Johannesburg. These data must be cross checked with updated data from the delta such as cross sections, flow discharges, sediment rates, slopes, etc.

Sediment Formulae

The measured bedload data from the Panhandle should be tested against existing bedload or total load sediment formulae such as Meyer-Peter&Müller and Engelund-Hansen. McCarthy et al have developed a special sediment transport formula for the Okavango Delta, which should be compared to the formulae mentioned above. The derived formula is based on relatively few data from 1987-1988 and from 1991, and is not necessarily representative for the entire delta, and for a long term. Thus, changes to the sediment formula may be envisaged. The output is one updated (or unchanged) sediment transport formula, which is valid not only for low and medium flow but also extreme high flow.

Cross Sections in Panhandle

All cross sections in the upper Panhandle should be critically analysed and checked regarding the time of survey, the consistency from one cross section to another, the slope, the average conveyance at difference flow stages, etc. Any significant and inexplicable deviations in the cross section parameters will be reflected and amplified in erroneous sediment transport results. The output is one set of modified and corrected cross sections of the Okavango River in the Panhandle, with due consideration that the river is divided into parallel branches in certain places. The river model should, however, only have *one* representative branch. The cross sections may therefore require some adjustment.

Time Series

Sediment transport is a highly non-linear function of the flow discharge. Thus, the majority of the sediment transport takes place during a few large flood events. Therefore it is necessary to investigate available historic discharge time series to identify determining historic big flood events causing extraordinary high sediment inflows and/or redistribution in the delta. A 50 year period is envisaged to be the minimum time horizon (meaning that the flood event with a 50 year return period should be identified).

Catchment Sediment Yield

Trends of changes in the sediment yield (soil erosion) from the upstream catchment should be identified. This could be based on accessible study reports of river basin developments in the riparian countries, and similar evidence of changes in land use, agriculture, urbanisation, river bank protection or river training, damming, etc.

Analytical or Conceptual model

The physical processes to be considered (long term shifts in distributary channels, short term variations in channel morphology, channel-flood plain interaction, channel avulsion, and impact of dredging), should initially be described in conceptual models. This must be done prior to actual modelling with the integrated surface-ground water hydrologic model in order to avoid misuse and misinterpretation of study results. These results are partly summarised in the section on Key Characteristics above.

Conveyance Analyses

The long term processes will be based on interpretation of the longitudinal variation along the Thaoge, Jao-Boro, and Nqoga-Maunachira of the flow conveyance, the sediment transport conveyance and the slope. From this, the risk of shifts in the future given the present channel geometry along each reach can be assessed. Furthermore, by calculating the sediment inflow at the upstream reaches of each primary distributary channel, the future channel geometry (existing shape + new slope) may be applied for the assessment of risks of shifts.

Finally, the fan should be distributed into three or four subareas around each main distributary and extending from the apex down to the downstream end of the fan. The overall average gradient over the flood plain-swamp-terrain in each sub-area should be assessed (from the Topographic Model). In this manner, the process of possible channel avulsion is taken into account.

Channel-Flood Plain Interaction

The short term processes, and in particular the overspill and seepage of flow from the channel to the flood plain causing loss of sediment transporting capacity in the channel and subsequent aggradation, should be described for different reaches. This is done by comparing the flow transport capacity (conveyance) of the main channel for different water stages, and comparing this with the actual flood plain level as well as the simulated flow in the main channel. In principle, the flow conveyance along eg Nqoga can be plotted as a function of chainage. Also the sediment transport capacity along Nqoga can be plotted. From this, potential areas of overspill as well as sedimentation (river bed aggradation) can be identified and compared with the actual observations from the field.

Sediment Transport Model

Although morphological feedback can be incorporated, it will not be used for the entire integrated model of the delta for two reasons. Firstly, the "predictive power" of a one dimensional channel and sediment transport model is very limited in the split points. Secondly, the overall integrated ground-surface water hydrologic model is designed for short term (up to a few decades) simulations, whereas true morphological simulations require model discretisations (such as topographic description) prepared for long term assessments.

Long Term Panhandle MIKE 11 Model (Model 3)

The upper part of the delta, the Panhandle, should be simulated in morphological mode in order to address the long term time scale and length scale of the impact of different upstream boundary conditions. In order to have a model which can run for 50 years, the ground water component will be excluded, and alternative ways to represent water losses in the MIKE 11 model of the Panhandle will be used. The morphological divide level of cross sections will be adjusted until the channel conveyance is reasonable uniform down through the Panhandle. (This is a reasonable assumption as the river is unregulated over decades and centuries.)

Short Term Fully Integrated MIKE SHE-MIKE 11 Sediment Model (Model 2)

In the primary flow channels, there is a balance between flow, overspill per unit channel length, width decrease per unit channel length, change in slope along the river, river bed aggradation (or degradation) and sediment transport rate. In the model, this balance is relying on accurate representation of the primary channels through the few model cross sections with eg 10-20km spacing. It is envisaged that the accuracy or representation is limited, and some adjustment of cross sections based on morphological insight may be required. The MIKE 11 model for the MIKE SHE coupling has a 1km extra band along either side of the channel representing part of the flood plains.

This will obviously cause an overestimation of the in-channel flow. This is compensated by using the "Morphological divide level" in the cross section data base. The divide level virtually divides the total cross section discharge into a flood plain discharge (overland flow parallel to the river) and a channel discharge. The morphological divide level becomes a calibration parameter, which needs to be adjusted within reasonable limits until the flow (and sediment) conveyance exhibit a uniform (stable, increasing or decreasing) pattern along the river channel. Some of the MIKE 11 branches in the setup can be defined as morphologically "passive branches" meaning that the sediment transport computation is excluded in these branches. In this manner, only the specific areas of particular interest can be defined as morphologically active.

Short Term Fully Integrated MIKE SHE-MIKE 11 Hydraulic Model (Model 1)

The impact of major channel shifts in terms of changed flooding patterns can be simulated with the existing integrated model (MIKE SHE-MIKE 11) without sediment transport. The channel is adjusted or excluded from the existing model prior to such scenario simulations. The corresponding probability of such major channel shifts is found through desk studies of the conveyance along each distributary.

Extension of Model to Popa Falls

For sediment transport simulations, an accurate upstream boundary condition is required. This may be either a time series of sediment transport, or a fixed bed elevation. The latter is well defined at the Popa Falls, where it can be assumed that the rock bed is fixed. The boundary condition is particularly important, when scenarios like construction of upstream dams are simulated. Therefore, the surface water model should extend further upstream

than the groundwater model in the integrated MIKE SHE-MIKE11 model. Upstream cross sections are required for the extension. They must be quality checked. The output is an improved model setup, which facilitates sediment transport simulations.

ANALYSES

Long Term

The main analyses related to long term river processes to be dealt with in the study are:

- Theory about alluvial fans. The simplified MIKE 11 model of the Panhandle (model 3) using morphological update can be used to address time scales. This could be done as part of a training course for the modelling unit.
- Okavango River Catchment, Assessment of soil erosion. Past, present, future. This should be done on the basis of a brief review maps of vegetation, land use, etc as described in the section on Data Processing and Interpretation.
- Annual inflow of sediment. Check of McCarthy's sediment formula using MIKE11 sediment models as described.

Short Term

The main analyses related to short term river processes, which should be carried out in the study, are as follows:

- Theory about bed form migration. Pulses of sediment. The MIKE 11 model of the Panhandle (model 3) can be used to analyse the importance of extreme flood events in terms of morphology.
- Flow distribution. Check MIKE SHE-MIKE 11 predictions against measurements. Improve MIKE 11 sub-model focussing on channel flow especially (cross section and alluvial resistance). The use of the "morphological divide level" is required in this respect. This parameter must be set for each cross section, so that a reasonable uniform longitudinal variation in transporting capacity is obtained.
- Theory about vegetation impact on channel forming processes. Reference to McCarthy's papers. In addition, ODMP should propose further scientific research work.
- Calculate sediment distribution with the MIKE 11 model of the entire Okavango Delta area. Without coupling to "vegetation morphology" and therefore also without bed level updating (morphological update). This analysis will only show the potential sediment transport capacity.
- Discuss state of equilibrium. Recent channel avulsion causing a system out of equilibrium (channels with aggradation or degradation). This should be based on the analysis of channel parameters along the entire reach of each primary channel, see section on Analytical or Conceptual Model.

SCENARIOS

Consequences

The impacts of the various water resources development scenarios on the delta morphology may be assessed by:

- Identifying possible channel shifts with given probability. Use of the analytical model of sediment carrying capacity.
- Calculate "what if" scenarios: Nqoga closing, (and Jao and Thaoge). Use of the integrated surface-ground water hydrologic model with changed MIKE 11 cross sections and without sediment transport computations (Model 1)
- Calculate the time before significant upstream changes in the catchment have an impact on the Okavango Delta downstream of the Panhandle. With the simplified MIKE 11 Panhandle model (Model 3)

Management and Intervention Options

The impacts of the various management and intervention options on the delta morphology may be assessed by:

- Monitoring. External changes. Propose routine measurements at Mohembo (direct indicators).
- Monitoring. Internal changes. Propose "special surveys" in the main distributaries: Cross sections and flow (indirect indications).
- Impact of unblocking channels (weed cutting). Use of the integrated surface-ground water hydrologic model covering the entire study reach and with sediment transport and bed level updating in the computations for specific reaches (Model 2). The model will show the extent of the impact area (and the change in time), both the hydraulic and hydrological impact, as well as the morphological impact (enhanced erosion etc)
- Impact of dredging existing channel, or cutting a new channel (connection). Use of the integrated surface-ground water hydrologic model covering the entire study reach and with sediment transport and bed level updating in the computations for specific reaches (Model 2).